Journal of Hydrology: Regional Studies 42 (2022) 101143

Contents lists available at ScienceDirect

Journal of Hydrology: Regional Studies

journal homepage: www.elsevier.com/locate/ejrh

Variability and changes in hydrological drought in the Volta Basin, West Africa

Solomon H. Gebrechorkos [a,*], Ming Pan [b,c], Peirong Lin [b], Daniela Anghileri [a], Nathan Forsythe [d], David M.W. Pritchard [d], Hayley J. Fowler [d], Emmanuel Obuobie [e], Deborah Darko [e], Justin Sheffield [a,b]

[a] School of Geography and Environmental Science, University of Southampton, Southampton, United Kingdom
[b] Department of Civil and Environmental Engineering, Princeton University, Princeton, NJ, USA
[c] Center for Western Weather and Water Extremes, Scripps Institution of Oceanography, University of California San Diego, La Jolla, CA, USA
[d] School of Engineering, Newcastle University, Newcastle upon Tyne, United Kingdom
[e] Water Research Institute Council for Scientific and Industrial Research (CSIR), Ghana

ARTICLE INFO

Keywords:
Hydrological extremes
Droughts, Volta basin, Drought propagation
Severity
Streamflow

ABSTRACT

Study region: Volta River Basin, West Africa
Study focus: Hydrological droughts have a wide range of impacts on societies and economic sectors such as agriculture and energy production. Analysis of hydrological droughts helps better plan and manage water resources under global change. This study analyses the spatial and temporal variability of hydrological drought occurrence (duration and severity) in the Volta River basin during 1979–2013. We used the Variable Infiltration Capacity and vector-based routing (RAPID) models and high-resolution forcing data to simulate streamflow for 10300 river reaches.
New hydrological insights for the region: Drought duration and severity show high spatial variability and large differences between the three decades (1980 s, 1990 s and 2000 s). Droughts are more severe in larger catchments as the flows are generally higher. The trend analysis shows a general decreasing trend (up to 5% per event) in drought duration in the north-eastern and an increasing trend in southern parts of the basin. Drought severity shows an increasing and decreasing trend (up to ± 20%) in south and north part of the basin, respectively. Daily streamflow has a maximum correlation (up to 0.78) with upstream precipitation for the previous 30-days with a clear signal of propagation from meteorological to hydrological drought with an average lag-time of two weeks. The results indicate the need to consider site-specific and adaptive drought management measures to minimize the impacts.

1. Introduction

Drought is a complex and recurrent climatic phenomenon that affects the environment, economies and a large number of people globally every year (Wilhite et al., 2007; Sternberg, 2011; IPCC, 2012; CRED, 2018). The most negative impacts usually occur in developing countries where droughts can lead to crop failure and food crisis. Together with other socio-economic conditions, droughts can amplify the risk of malnutrition, health issues, and chronic poverty, which may ultimately result in forced migration and even loss

* Corresponding author.
E-mail address: shg1f19@soton.ac.uk (S.H. Gebrechorkos).

https://doi.org/10.1016/j.ejrh.2022.101143
Received 7 March 2022; Received in revised form 9 June 2022; Accepted 11 June 2022
Available online 17 June 2022

of life (Vicente-Serrano et al., 2012; Lyon and DeWitt, 2012; Stanke et al., 2013; UNISDR CRED, 2015; Haile et al., 2020; Ngcamu and Chari, 2020). Drought occurs across a wide range of spatial and temporal scales, which makes managing socio-economic and environmental impacts such as land degradation and desertification very challenging (Vicente-Serrano et al., 2012; Masih et al., 2014; Rivera et al., 2017). Variation in drought characteristics is driven by variability and changes in precipitation and temperature (IPCC, 2012), but can also be aggravated by direct anthropogenic drivers such as water management and land-use (Mishra and Singh, 2010; Sheffield et al., 2012; Mukherjee et al., 2018). Global warming and an increase in temperature extremes have increased concurrent extreme events such as heatwaves and droughts (AghaKouchak et al., 2014; Ballarin et al., 2021; Leonard et al., 2014). The potential impact of this type of compound event could lead to longer and more severe hydrological droughts. As a result of increased variability and long-term changes in climate, the duration and severity of droughts have potentially increased in Africa in the last few decades (Sheffield et al., 2012; Dai, 2013; Sivakumar et al., 2014; Naumann et al., 2018). This is expected to continue into the future, as drought magnitude and severity are projected to increase under global change (IPCC, 2013; Naumann et al., 2018; Sheffield and Wood, 2008), with the largest changes expected in sub-tropical dry regions that are projected to become drier overall. Droughts are already common in arid and semi-arid regions of Africa and their frequency and duration has increased in recent years, such as in West Africa (Dai, 2013; Masih et al., 2014) and the Greater Horn of Africa (Sivakumar et al., 2014; Ayana et al., 2016; Nicholson, 2017; Haile et al., 2020). For Africa, overall, future climate projections indicate an increase in frequency and intensity of droughts as well as other extreme events such as floods and heavy rainstorms (Bates et al., 2008; Niang et al., 2014; Gebrechorkos et al., 2019).

Many African countries face the highest impact of drought due to their lower capacity to adapt to changes (Niang et al., 2014; McDowell et al., 2016). They are also likely to be increasingly impacted in the future, not only because of the projected changes in drought but also because of ongoing socio-economic changes. Over the last few decades, the demand for water has significantly increased by many folds and water scarcity is occurring almost every year, due to an increase in population growth and expansion in agriculture, industrial, and energy sectors (Mishra and Singh, 2010). The increase in population and economic activities have led to an increase in construction of water infrastructure to meet sectoral demands, which put water resources under increasing stress (Mul et al., 2015).

According to Haile et al. (2020), assessing drought risks at a basin level is crucial to effectively and efficiently monitor and manage droughts, and can serve as a basis for development of adaptation measures under conditions of climate variability and change (Oloruntade et al., 2017). The current study focuses on one of the largest river basins in West Africa, the Volta basin, aiming to provide a detailed analysis of the variability and change in hydrological drought, focused on streamflow. The analysis is carried out using modeled data over an unprecedented number of river reaches (i.e. 10,300). The Volta River basin is an important resource for around 24 million people across six countries (Ghana, Burkina Faso, Mali, Ivory Coast, Benin, and Togo) using water for domestic, livestock, agriculture, and hydropower purposes (Rodgers et al., 2007; Mul et al., 2015). The basin, therefore, plays an important role in the economic development of the region. However, due to increases in demand from the increasing population and economic growth, there is potential for competition over water resources that are already under stress, which is exacerbated under drought conditions (Mul et al., 2015). This is expected to become worse in the future with consequences for the food security and economic growth of the six countries (Mccartney et al., 2012; Mul et al., 2015).

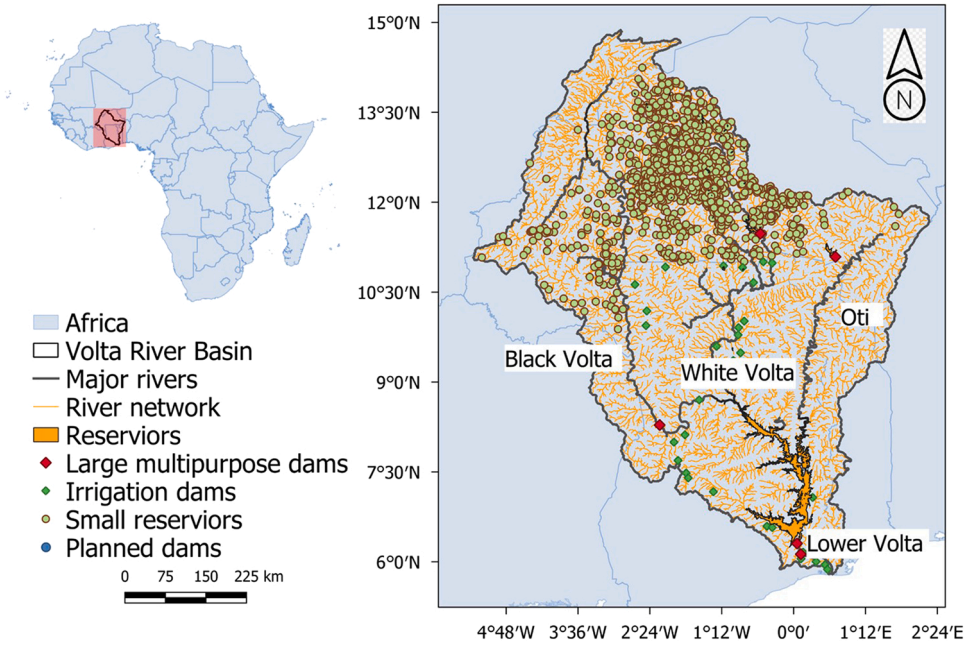

Fig. 1. Location map of the Volta River basin and location of reservoirs (large multipurpose, irrigation, and small impoundments) and planned dams.

We focus on the characterization of streamflow droughts over the period 1979–2013, in terms of the time below a threshold level (drought duration) and accumulated streamflow deficit (drought severity), which is derived from the streamflow time series (e.g., Melsen and Guse, 2019; Rivera et al., 2017). We choose this period due to the availability of the most reliable precipitation data, which begins at the start of the satellite period. We also assess the relationship between daily streamflow and antecedent precipitation, and therefore how meteorological droughts propagate into hydrological droughts. Because of the lack of coverage in time and space of observed records of streamflow, we use simulated runoff from the Variable Infiltration Capacity (VIC) land surface hydrological model (Liang et al., 1994). Further, we used the Routing Application for Parallel Computation of Discharge (RAPID) routing model (David et al., 2011) to convert the runoff from VIC into streamflow. These simulations are forced by a gridded gauge-satellite-reanalysis climate forcing dataset. We compare the modeled streamflow against available observations of streamflow to understand the performance of the model and its suitability for looking at drought characteristics across the basin. Overall, the analysis could provide baseline risk information for users and water agencies to better manage water resources, develop site-specific adaptation measures and support the development of integrated water management and planning strategies to tackle the impacts of droughts under variability in climate and future change.

2. Material and methods

2.1. Study area

The Volta basin is one of the largest river basins in West Africa with an area of 412,772 km^2 (Fig. 1). The basin is shared among Burkina Faso (43.0% of the basin area), Ghana (41.6%), Togo (6.4%), Benin (3.4%), Mali (3.1%), and Côte d′Ivoire (2.5%) (Mul et al.,

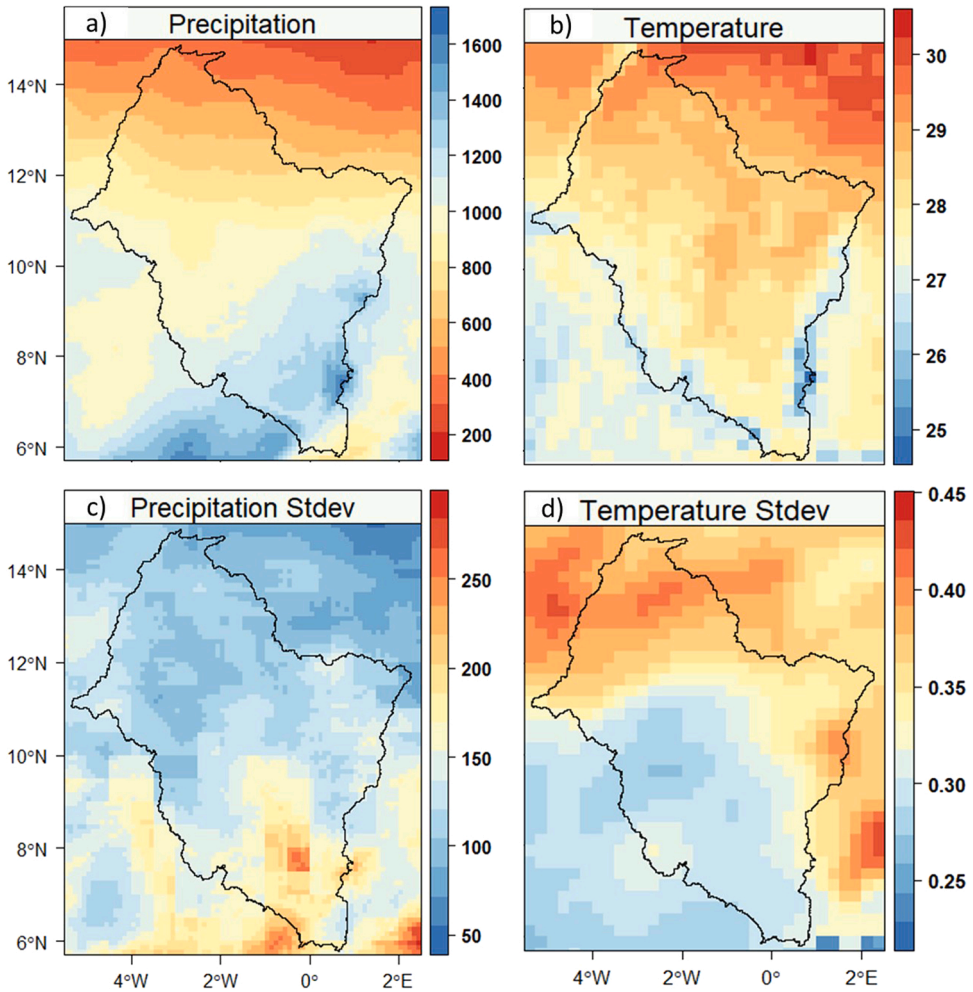

Fig. 2. Maps of (a) annual average (1979–2013) precipitation (mm/year) and (b) average temperature (°C/year) of the Volta basin based on the Multi-Source Weighted-Ensemble Precipitation (MSWEP) and Princeton Global Forcings (PGF) (see Section 2.3), respectively. The lower maps show the standard deviation (Stdev) of (c) annual precipitation and (d) average temperature for the period 1979–2013.

2015). The Volta has four major sub-basins: White Volta, Black Volta, Lower Volta, and Oti River covering an area of 27%, 36%, 18%, and 19% of the total drainage area, respectively (Gordon et al., 2013; Mul et al., 2015). The climate is highly variable, with a clear gradient from south to north as influenced by the movement of the Intertropical Convergence Zone (ITCZ) and zonal winds, which leads to high variability in floods and droughts. The climate of the river basin is classified as moist sub-humid, dry sub-humid, and semi-arid in the south, central and north, respectively (Ferreira et al., 2019; Mul et al., 2015). More than 1100 reservoirs (large multipurpose, irrigation, and small impoundments), with a storage volume of between 1 and 147,960 Mm^3, have been constructed during the 1980–2010 s. There are 19 planned hydropower dams in the basin due to an increase in water demand for energy, agriculture and water supply (Barry et al., 2005; Mul et al., 2015).

The average annual precipitation for the basin over 1979–2013 is 850 mm/year with the highest and lowest amounts in the southern (up to 1600 mm/year) and northern (up to 400 mm/year) parts of the basin, respectively (Fig. 2a). The inter-annual variability of precipitation is higher in the Lower Volta (standard deviation up to 250 mm) but decreases towards the northern part of the basin (Fig. 2c). On average, the basin receives about 70 % of the total precipitation during July-September with little rainfall during the months of November-March. The northern part receives the majority of precipitation during June-September while the southern part receives this during May-September (Jones et al., 2017). The northern part is warmer than the southern part with an annual daily average (1979–2013) temperature of about 29 °C (Fig. 2b). Inter-annual variability in average temperature is higher in the north (standard deviation up to 0.43 °C) and lower in the south (standard deviation up to 0.23 °C) part of the basin (Fig. 2d).

2.2. Hydrological modelling and streamflow routing

The VIC model is a semi-distributed model that solves the energy and water balances at the grid-scale (Liang et al., 1994). VIC organises the spatial domain into different computational cells characterized by land cover type and vertically into soil layers to calculate water budget components such as runoff (surface and subsurface), evapotranspiration and infiltration. The horizontal flow between grid cells is not modeled and it is assumed that water cannot flow back into the soil after reaching the river (Dang et al., 2020). The Penman-Monteith approach is used to compute evapotranspiration. The variable infiltration curve is used to represent the spatial distribution of infiltration and surface runoff within the grid cell, and the non-linear Arno-recession curve is used for baseflow simulation (Liang et al., 1994). The variable infiltration curve is an important part of VIC which drives the partitioning of rainfall into infiltration and runoff depending on the spatial distribution of soil moisture. Meteorological forcings required by VIC are daily precipitation, temperature, shortwave and longwave radiation, wind speed, atmospheric pressure, and vapour pressure. In addition, soil (e.g., texture and bulk density, saturated conductivity) and vegetation (e.g., albedo and leaf area index) parameters are required to parametrize the model (VIC 4.2). The model is calibrated and bias-corrected at 0.25° to match global maps of 17 runoff characteristics such as mean annual runoff, baseflow index and different percentiles derived from ground observations (Beck et al., 2015). The most sensitive VIC parameters for runoff generation were calibrated such as the variable infiltration curve (b_{inf}), soil depth, and the maximum soil moisture fraction at which non-linear (rapidly increasing) baseflow begins (Ds). The observation-based runoff maps were developed to estimate streamflow at ungauged catchments and more than 3000 stations were used to train a machine learning (neural network ensembles) and applied globally (Beck et al., 2015). The use of these runoff characteristics improved the performance of hydrological models in simulating streamflow as compared to traditional calibration approaches using limited ground stations (Lin et al., 2019).

RAPID (David et al., 2011) is a vector-based routing model used to simulate streamflow at potentially thousands of river reaches. It applies the Muskingum channel routing scheme to calculate the volume of water and streamflow, with dimensionless (x) and time (k) parameters. In addition, the model requires a network connectivity file and gridded runoff (surface and subsurface), which can be computed in Arc-GIS (eg., https://github.com/Esri/python-toolbox-for-rapid). To assess the performance of VIC/RAPID, the modeled streamflow is evaluated against available in-situ data on daily and monthly time scales in terms of the correlation coefficient (CC), percentage bias (Pbias), Root Mean Square Error (RMSE) and Nash-Sutcliffe Efficiency (NSE) and time series plots.

2.3. Datasets

Meteorological forcing data to drive the VIC model are taken from the Multi-Source Weighted-Ensemble Precipitation (MSWEP, Beck et al., 2016) dataset and from the Princeton Global Forcings (PGF) (Sheffield et al., 2006). MSWEP (version 2.2) is a global precipitation product developed by merging several datasets such as from more than 77,000 ground stations, satellite-based rainfall estimates, and reanalyses (Beck et al., 2018, 2016). The dataset has been shown to out-perform other similar precipitation products (Beck et al., 2017) and has been used in many regional and global hydro-climate studies (e.g., Chen et al., 2017; Chen and Dirmeyer, 2016; Liu et al., 2016; Martens et al., 2017; Schellekens et al., 2017). PGF is developed by combining the National Centers for Environmental Prediction–National Center for Atmospheric Research reanalysis data with several observational-based climate datasets such as the Climatic Research Unit monthly gridded gauge analysis dataset of temperature and humidity (New et al., 2000, 1999) and the Surface Radiation Budget satellite-based dataset (Barkstrom et al., 1989). PGF has proven to be a reliable dataset used in many hydro-climate studies (e.g., Troy et al., 2011; Wang et al., 2011; Demaria et al., 2012; Niko Wanders and Wood, 2016; Gebrechorkos et al., 2018, 2020).

The river network, required as input to RAPID, is taken from the 30-sec resolution “Hydrological data and maps based on SHuttle Elevation Derivatives at multiple Scales” (HydroSHEDS) dataset. HydroSHEDS provides a georeferenced vector and raster stream network and flow directions derived from the Shuttle Radar Topography Mission (SRTM) elevation data (https://hydrosheds.cr.usgs.gov/). The location of the reservoirs shown in Fig. 1 are obtained from the Water Research Institute of Ghana. Although we do not model the hydrological impact of the reservoirs and dam operations, we discuss the results in the context of their presence across the

basin. To assess the potential differences between the model output and (the unobserved) reality, we calculated the degree of regulation (DOR) as the ratio of the reservoir capacity to average annual flow upstream of the reservoir (Lehner et al., 2011) for each reservoir with available capacity information. For a given year, a higher DOR indicates the probability that a substantial amount of flow can be stored for future release, which influences flows downstream (Lehner et al., 2011). The DOR was then used to inform a qualitative assessment of the performance of the model where the lack of reservoir representation in the model could lead to large uncertainties or errors in the modelled output and drought characteristics.

Observed streamflow data from 39 stations (20 daily and 19 monthly) were obtained from the Global Runoff Data Centre (http://www.bafg.de/GRDC/) and the Water Research Institute of Ghana (Tables 1 and 2). The GRDC database provides quality-controlled historical daily and monthly streamflow to help scientists perform global and local scale hydrological and environmental studies (GRDC, 2019).

2.4. Drought indices and trend analysis

The threshold level approach (Yevjevich, 1967) is used to define streamflow droughts. The threshold is derived from the flow duration curve as flow exceeded or equalled for selected percentile thresholds: 70%, 80%, and 90% of the time. These thresholds are classified as moderate, severe, and extreme droughts, respectively (Rivera et al., 2017), which is an approach that has been widely used to assess streamflow droughts (e.g., Fleig et al., 2006; Wanders et al., 2015; Rivera et al., 2018). Compared to standardised indices such as the standardised streamflow index (McKee et al., 1993; Shukla and Wood, 2008), the threshold level approach allows estimation of streamflow deficit (severity), which is crucial for water management in sectors such as agriculture and hydropower (Rivera et al., 2018; Van Loon, 2015).

Streamflow droughts are computed from the daily time series of the modelled years (1979–2013) using the threshold approach. The approach defines droughts when the flow is below the given threshold value. The threshold values are computed based on a moving quantile, where daily threshold values are defined based on the 70th, 80th, and 90th percentiles of the flow duration curve over a moving window of 30 days that moves through the time series of the study period (Beyene et al., 2014; Dierauer and Whitfield, 2019). Hence, this method provides different threshold values for every day of the year, which remains the same across all years. This approach helps to account for the influence of seasonality. To identify individual droughts we used a minimum inter-event and event duration of 10 and 15 days, respectively, as recommended by the World Meteorological Organization (WMO, 2008) and (Dierauer and Whitfield, 2019). The event duration avoids counting two adjacent droughts separated by minor fluctuations around the threshold as separate events. Droughts occurring with less than the minimum inter-event days (i.e., 10 days) were considered as a single event. Droughts are assessed in terms of their duration (days) and severity (m^3/s). Further, severity and total severity (total deficit volume during the drought events) are normalised by mean annual flow and catchment area for spatial comparison. The moderate, severe and extreme droughts are assessed relative to their threshold level. This does mean that a moderate drought may contain a severe or extreme drought if values fall below the threshold for these latter types of drought. To assess the presence of monotonic downward or upward trends in drought duration days and severity, we used the Mann-Kendall test (Kendall, 1975) and the magnitude of the change (i.e., slope) is computed using the Sen's slope method (Sen, 1968).

Furthermore, we assessed the propagation of drought (i.e. meteorological to hydrological droughts) via the relationship between precipitation and streamflow, to understand the influence of precipitation variability on the changes in hydrological drought. We calculated the 3, 7, 14, 21, 30, 60, and 90 days moving average of antecedent precipitation averaged over the upstream catchment, for

Table 1
List of stations with daily records during the period 1979–2013.

No	Station	Location		Upstream Area (km^2)	Period	Missing days (% missing)
		Lat.	Lon.			
1	Prang	7.98	-0.88	6355	1998–2006	367 (11.1)
2	Bamboi	8.15	-2.03	134,200	1980–2006	5862 (59.4)
3	Ekumdipe	8.47	-0.22	6810	1979–1995	3926 (63.2)
4	Vonkoro	9.19	-2.71	111,500	1979–1992	4428 (86.6)
5	Sabari	9.28	0.23	58,670	1995–2005	576 (14.3)
6	Lama Kara	9.53	1.18	1560	1979–1982	398 (27.2)
7	Nawuni	9.7	-1.08	92,950	1979–2007	25 (0.2)
8	Porga	10.2	0.97	22,280	1979–1992	3070 (60)
9	Yagaba	10.23	-1.28	10,600	1995–2006	2450 (55.9)
10	Wiasi	10.33	-1.35	9500	1989–2006	3670 (55.8)
11	Pwalagu	10.58	-0.85	63,350	1975–2007	5320 (53.9)
12	Lawra	10.63	-2.91	93,820	1979–2007	4437 (45)
13	Tiele	10.72	1.2	836	1979–1992	3437 (67.2)
14	Nangodi	10.87	-0.62	11,570	2004–2007	35 (2.4)
15	Dan	10.92	-3.65	6345	1979–1983	180 (9.8)
16	Yarugu	10.98	-0.4	41,550	1998–2006	690 (21)
17	Samboali	11.28	1.02	4560	1979–1983	436 (23.8)
18	Samandeni	11.47	-4.47	4580	1979–1983	162 (8.8)
19	Dakaye	11.78	-1.6	4540	1979–1983	5 (0.27)
20	Yilou	13	-1.55	10,100	1979–1982	71 (4.8)

Table 2
List of stations with observed monthly streamflow data during 1979–2013.

No	Station	Stations		Upstream Area (km^2)	Period	Missing months (% missing)
		lat	lon			
1	Bagre	11.25	-0.33	33,120	1979–1990	7 (4.9)
2	Banzo	11.32	-4.82	2816	1979–1986	27 (28.4)
3	Batie	9.98	-2.90	5630	1979–1985	3 (3.6)
4	Bissiga	12.75	-1.15	16,965	1979–1985	3 (3.6)
5	Bittou	11.18	-0.28	4050	1979–1985	10 (12)
6	Boromo	11.78	-2.92	37,140	1979–1991	4 (2.6)
7	Dapola	10.57	-2.92	66,540	1979–1991	0 (0)
8	Diebougou	10.93	-3.17	12,200	1979–1986	15 (15.8)
9	Manimenso	12.75	-3.40	20,000	1979–1983	0 (0)
10	Niaogho	11.77	-0.75	30,200	1979–1985	7 (8.4)
11	Nobere	11.43	-1.18	7600	1979–1990	3 (2.1)
12	Noumbiel	9.68	-2.77	79,700	1979–1985	15 (18.1)
13	Nwokuy	12.52	-3.55	14,800	1979–1988	0 (0)
14	Ouessa	11.02	-2.82	50,820	1979–1986	8 (8.4)
15	Senchi	6.20	0.10	394,100	1979–1984	0 (0)
16	Tagou	11.15	0.62	5640	1979–1987	0 (0)
17	Tenado	12.17	-2.82	23,700	1979–1985	0 (0)
18	Wayen	12.38	-1.08	20,880	1979–1987	0 (0)
19	Yakala	11.35	-0.75	33,000	1979–1984	15 (21.1)

catchments smaller than 100 km^2, and identified the duration of antecedent precipitation with maximum correlation with streamflow variability. The selection of smaller catchments is to reduce the impact of flow travel time and spatially variable precipitation in larger catchments, which will affect the relationship between antecedent precipitation and streamflow. We then used percentile thresholds as above to identify the start of meteorological and hydrological droughts, and calculated the time lag between them as a metric of propagation.

3. Results

3.1. Comparison of observed and modeled data

The modeled streamflow data is compared with observed data using the methods described in Section 2.2. The performance of the model, in general, is very good (e.g. CC up to 0.96) and increases from daily to monthly time scale. Fig. 3 provides a summary map of the accuracy of the modeled data compared to station data at daily and monthly scales. Even though there is a high impact of large reservoirs and dams on the performance of the model, such as the Akosombo dam with a DOR of greater than 250 %, there is no clear relationship between the skill and DOR. The DOR ranges from 0.1 % to 552 %. The large reservoirs (> 2000 Mm3) show the highest DOR (>36 %) compared to the smaller reservoirs.

The monthly correlation at the basin outlet (most southerly station in Fig. 3b) is 0.2 because of the significant influence of the Akosombo and other upstream dams that are not accounted for in the model, but generally increases upstream and where there are fewer dams. The DOR of the Akosombo dam is about 270 %, which is consistent with the known and significant impact on downstream flow. Similarly, the Pbias and RMSE are higher at the outlet but lower at stations with few or no dams upstream. For example, at station Tile (no upstream dam), the monthly CC, Pbias, and RMSE, and NSE are 0.89, 0.7 %, 4.3 m^{3}s^{-1}, and 0.78, respectively. Moreover, for stations with the longest records and fewer data gaps, the modeled data capture the daily and monthly low and high flows very well, as shown for stations Nuwani (Fig. 4a) and Bittou (Fig. 4b), with CC and NSE values of 0.91 and 0.83 and 0.85 and 0.63, respectively. The reservoir above the station Nuwani have a DOR of about 36 % suggesting that their influence on the downstream flows recorded at these stations is relatively low. Overall, the monthly CC and NSE for most of the stations are higher than 0.7 and 0.55, respectively, and the reservoirs above these stations have a DOR of less than 36 %.

To evaluate the model performance for drought duration and severity, we identified seven stations with observed records of greater than 6 years (Fig. 5). The results indicate that the model does reasonably well in representing the average number of drought duration per drought event, but with a tendency to underestimate compared to the observations. This may be largely due to the impact of dams and reservoirs (e.g., because of the water storage and release for hydropower and diversion to agriculture), as well as uncertainties in the modelling. For example, at station Nawuni, the observed and modeled streamflow show average drought duration days of 66 and 41 for moderate, 72 and 42 for severe and 51 and 30 for extreme droughts, respectively (Fig. 5). The presence of upstream dams is expected to impact the drought regime downstream. Nevertheless, the reliability of the modeled data for drought analysis will be significantly lower in catchments with upstream dams and therefore we show the results in this context (Sections 3.3 and 3.4).

3.2. Simulated climatology of drought duration and severity

The spatial distribution of simulated drought duration and severity, averaged over all identified drought events during 1979–2013,

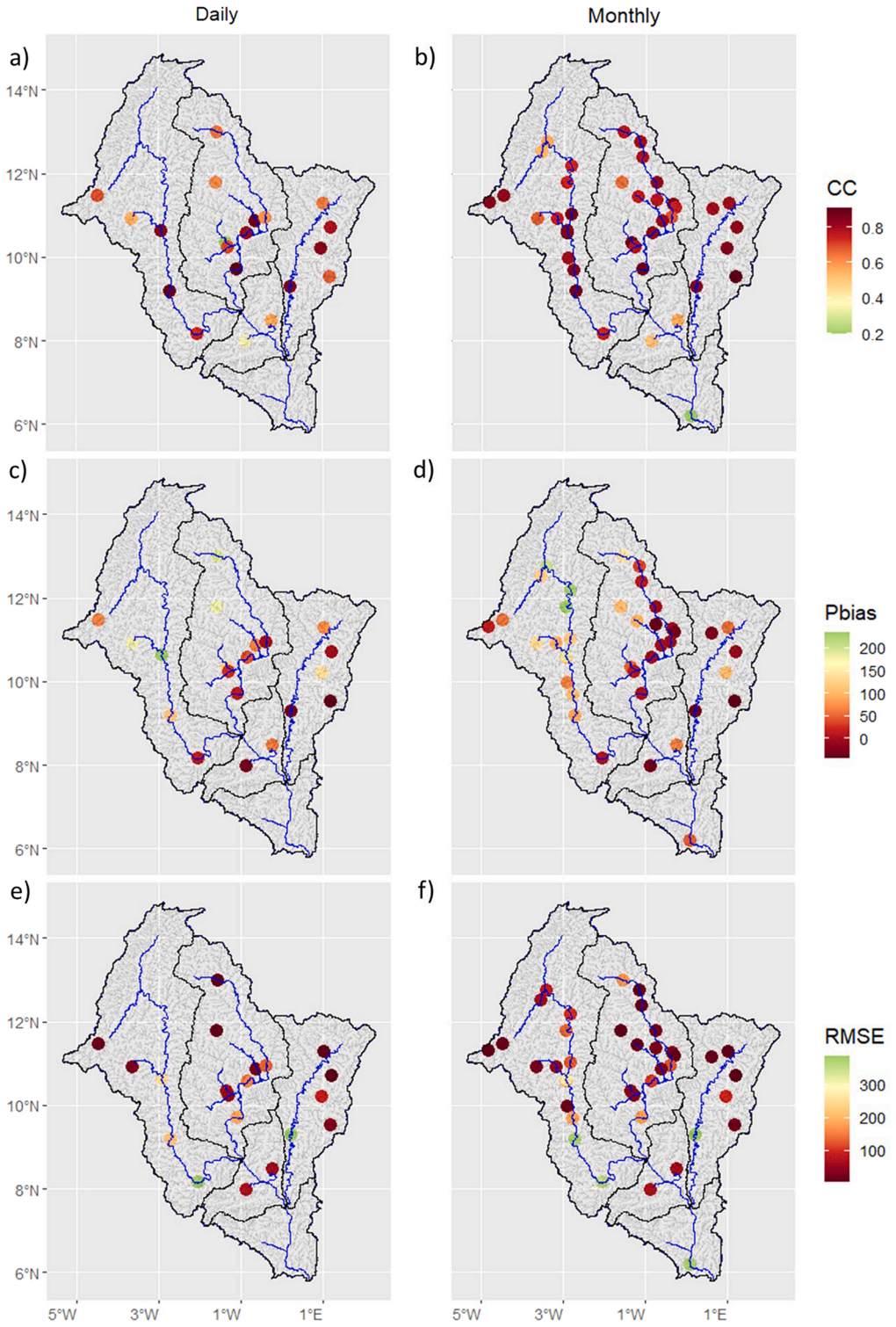

Fig. 3. Maps of evaluation statistics at daily (left) and monthly (right) scale for (a, b) correlation (CC), (c, d) Pbias (%), and (e, f) RMSE (m^3s^{-1}) of modeled streamflow compared to the observations. Darker red colours indicate better performance for each statistic. Blue and black lines show major rivers and catchments boundaries, respectively.

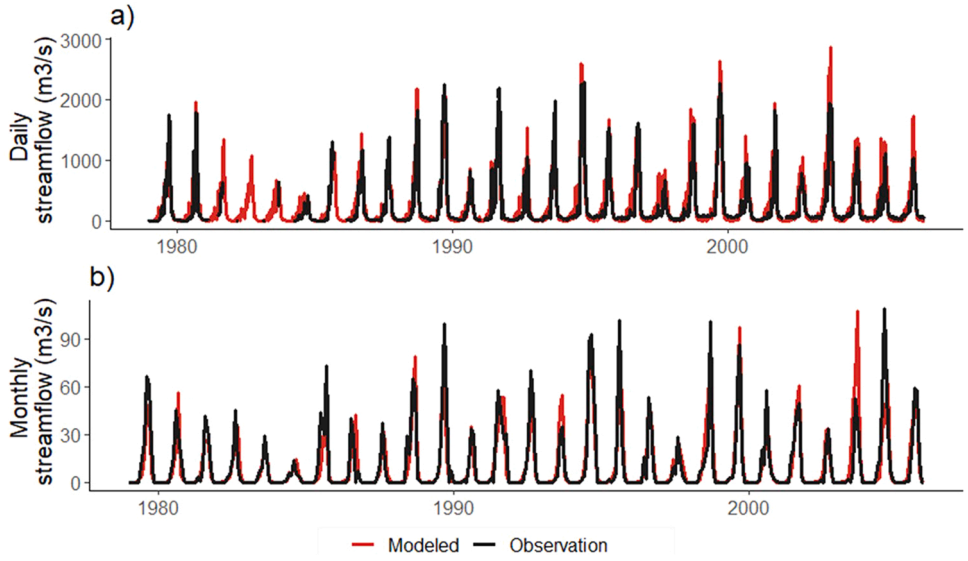

Fig. 4. Example time-series of observed and modeled streamflow at selected stations with long observational records: (a) Nawuni with available daily data, (b) Bittou with available monthly data.

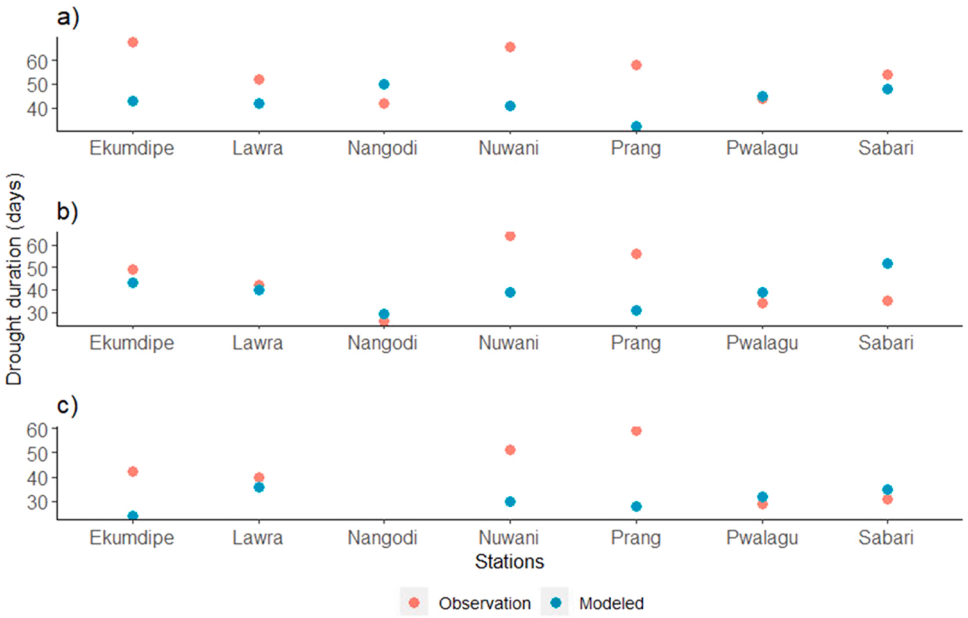

Fig. 5. Observed and modeled average drought duration (days) for moderate (a), severe (b), and extreme (c) droughts for selected stations with adequate observational data.

is shown in Fig. 6. The average drought duration is higher in the far south and northern parts of the basin for all threshold levels. Moderate drought durations (Fig. 6a) are lower (30–60 days) in the central part (8°N to 11°N) but higher (80–130 days) in the north, north-eastern and southern parts of the basin. Similarly, a lower number of severe (Fig. 6b) and extreme (Fig. 6c) drought durations (20–60 days) are simulated in central parts of the basin and increases towards the southern and northern parts of the basin (50–100 days). Moving from moderate to extreme droughts, drought duration decreases as expected but with hotspots of high drought durations persisting in the far north and south.

The normalised severity (severity divided by mean annual daily flow), is higher in the north and south-east (Fig. 6d-f), generally reflecting the spatial distribution of the drought duration but with also a west-east gradient with higher severity in the east. The severity for moderate droughts (Fig. 6d) is lower in large parts of the Black Volta and increases towards the northern part of the basin. The severity is higher in the Lower Volta, Oti River, and large parts of the White Volta, which shows an increase from the west to the

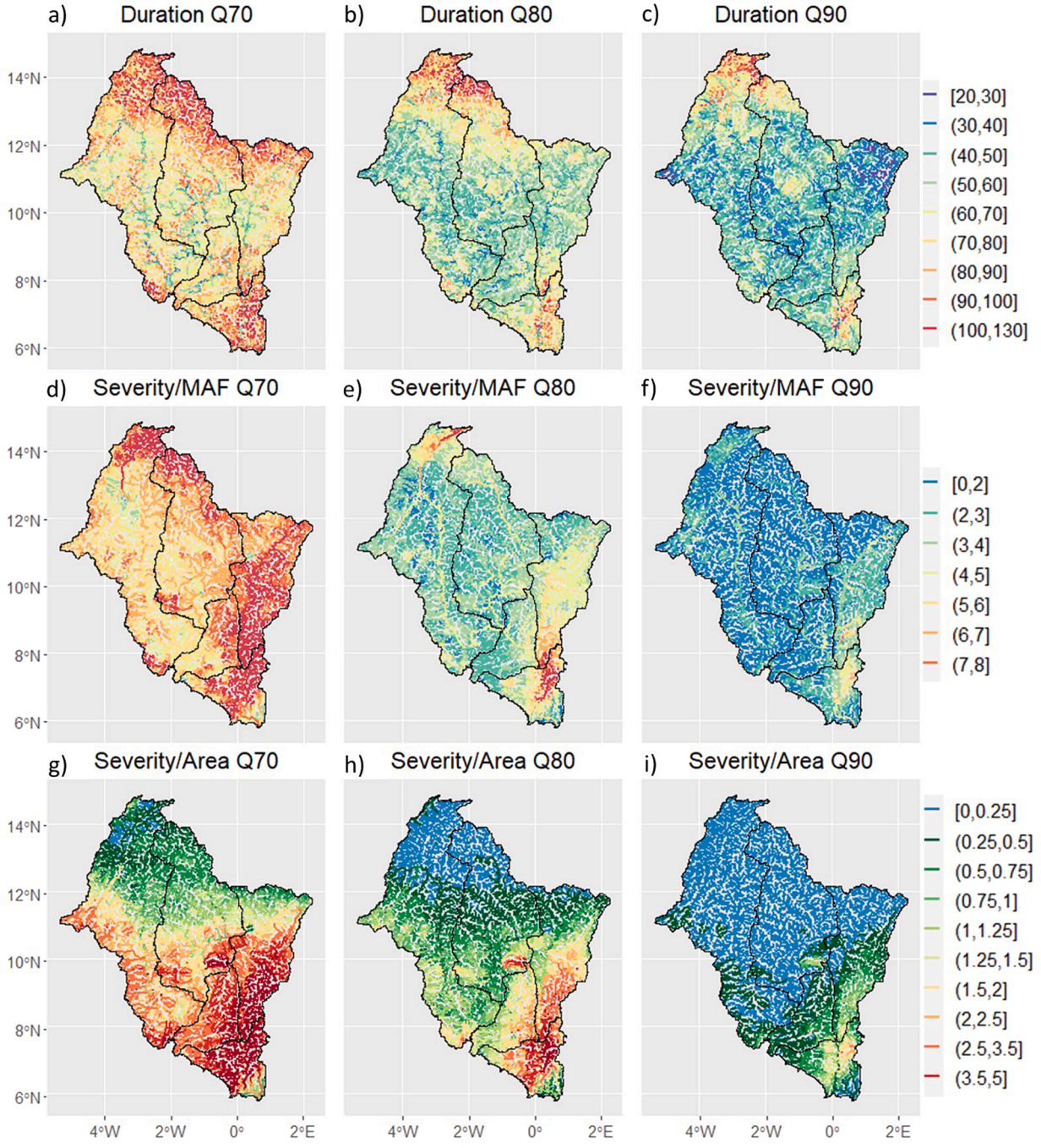

Fig. 6. Modeled average drought durations (a-c, days/event) and normalised severity (d-f, severity normalised by mean annual daily flow (MAF m^3s^{-1}/ m^3s^{-1})) and total severity (g-i, total severity normalised by catchment area (m^3s^{-1}/km^2)) for moderate (Q70), severe (Q80), and extreme (Q90) droughts during the period 1979–2013. Black lines show catchment boundaries.

east part of the basin. For severe droughts (Fig. 6e), similar to moderate droughts, the north part of the Black Volta, Lower Volta and the Oti River show a higher severity compared to the rest of the basin. Moreover, the Lower Volta and Oti River show a higher severity for extreme droughts compared to the Black and White Volta (Fig. 6f). In general, there is a tendency for longer drought durations and higher severity for river reaches with larger upstream areas, which is expected given the lower variability of flows (Fig. 6g-i).

Total severity normalized by upstream catchment area is lower in the upper part of the basin (< 0.25 m^3s^{-1}/km^2) and increases towards the Lower Volta (up to 5 m^3s^{-1}/km^2) with an increase in drainage area. For moderate (Fig. 6g), severe (Fig. 6h), and extreme (Fig. 6i) droughts, a large part of the Oti River shows the maximum severity (3–5 m^3s^{-1}/km^2) compared to the White and Black Volta.

Compared to moderate and severe droughts, the total severity for extreme droughts is lower in the White and Black Volta, with the maximum severity (up to 2 m^3s^{-1}/km^2) in the Oti River and Lower Volta.

Fig. 7 shows the same data as scatter plots and highlights the strong relationship between severity and catchment area, i.e. droughts are more severe in larger catchments as the flows are generally higher. The figure also shows the normalized severity (severity divided by MAF) versus catchment size, to account for this relationship, and shows that this becomes closer to a constant value (although dependent on the drought threshold) for catchments larger than about 2000–3000 km^2 (Fig. 7b). For smaller catchments, there is more diversity in values, which likely reflects the much higher variability of flows. Drought duration tends to vary for larger catchments from about 30–60 days depending on the threshold with a large range in values (from 30 to more than 120 days) in smaller catchments (Fig. 7c).

3.3. *Trends in drought duration and severity*

The trend analysis shows spatially varying trends over 1979–2013 in moderate, severe, and extreme drought duration and severity, with statistical significance in a few areas (Fig. 8). Relative to the long-term mean (Fig. 6a-c), the upper part of the White Volta and the Oti River show a decreasing trend in moderate and severe drought durations of up to 5% per drought event. Conversely, large parts of

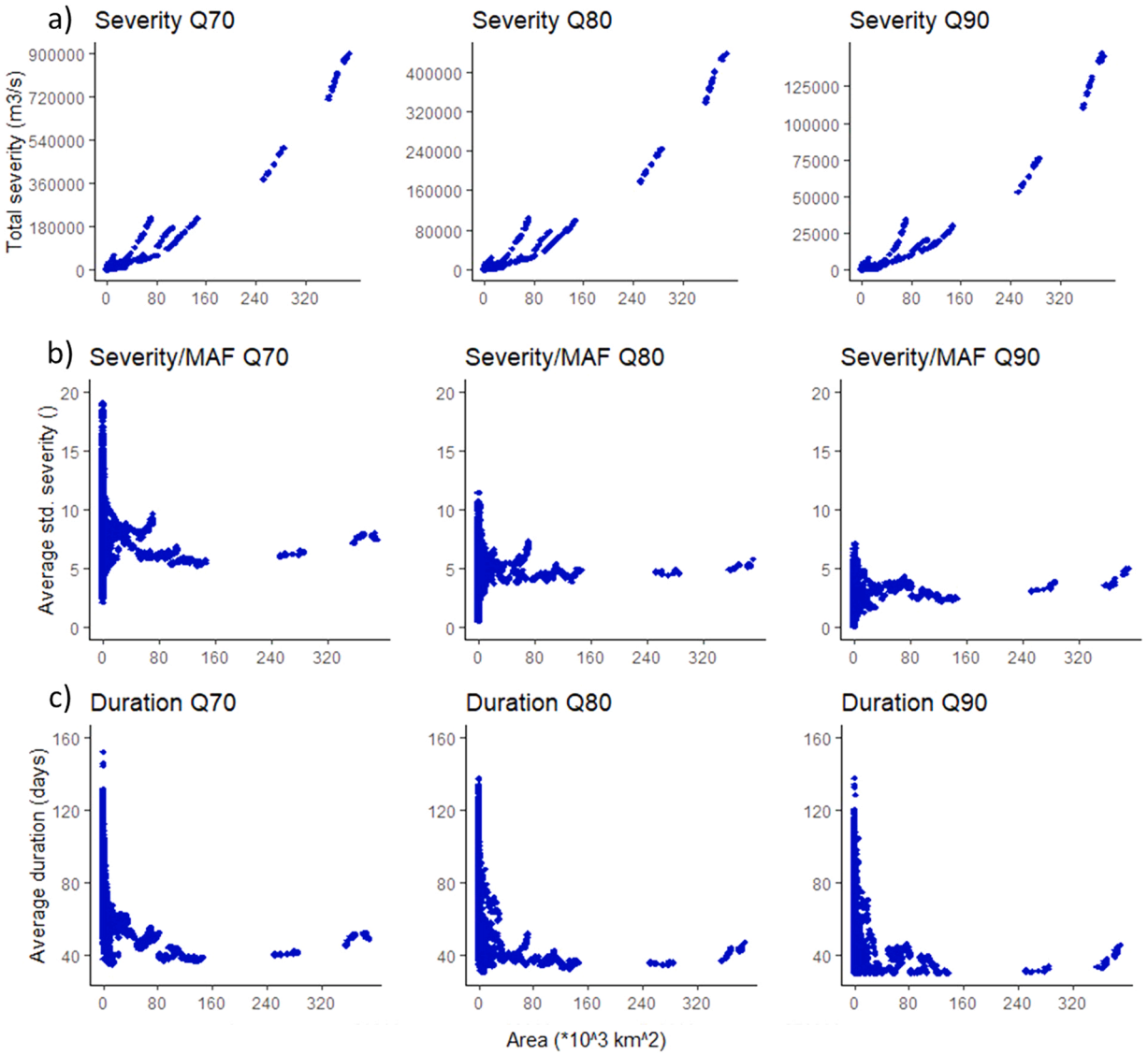

Fig. 7. (a) Upstream catchment area versus modeled total drought severity, (b) normalized severity (severity divided by MAF) versus catchment area, (c) drought duration versus catchment area for all river reaches for moderate (Q70), severe (Q80), and extreme (Q90) droughts during the period 1979–2013.

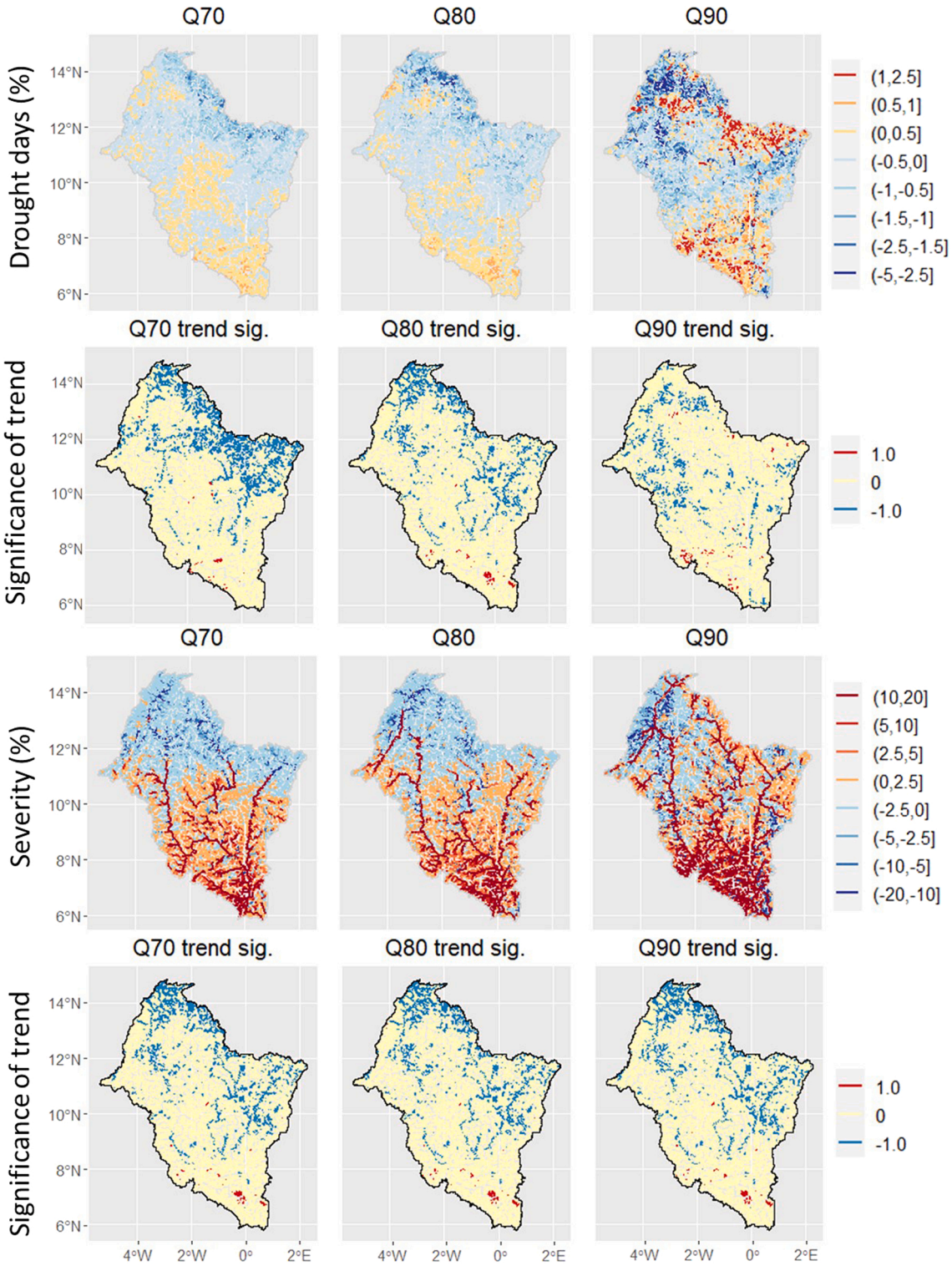

Fig. 8. Percentage of change, relative to the long-term mean (1979–2013), in moderate (Q70), severe (Q80) and extreme (Q90) drought duration and severity. The trend significance indicates significant increasing (1) and decreasing (−1) and non-significant (0) trend at P-value < 0.05.

the Lower and Black Volta and downstream of the White Volta show an increasing trend up to 1% per event. The decreasing trends in moderate drought durations in upstream parts of the White Volta and Oti River are statistically significant. The number of extreme drought duration days shows an increasing trend (up to 2.5% per event) in the upper parts of the White Volta and Oti River and large parts of Lower Volta, and a decreasing trend (up to 5% per event) in the Black Volta, which are significant in a few places.

Drought severity shows decreasing and increasing trends (up to ± 20% per event), significant in a few places, in the upper and lower parts, respectively, of the White Volta, Black Volta and Oti River, for moderate and severe droughts. The Lower Volta shows an increasing trend (up to 20% per event) for moderate, severe and extreme droughts. For severe droughts, a large part of the basin shows an increasing trend of severity, whereas the upper part of the Black Volta shows a decreasing trend of up to 20% per event. In general, drought durations and severity have decreased in the upper basin and increased in the lower basin, particularly for moderate and

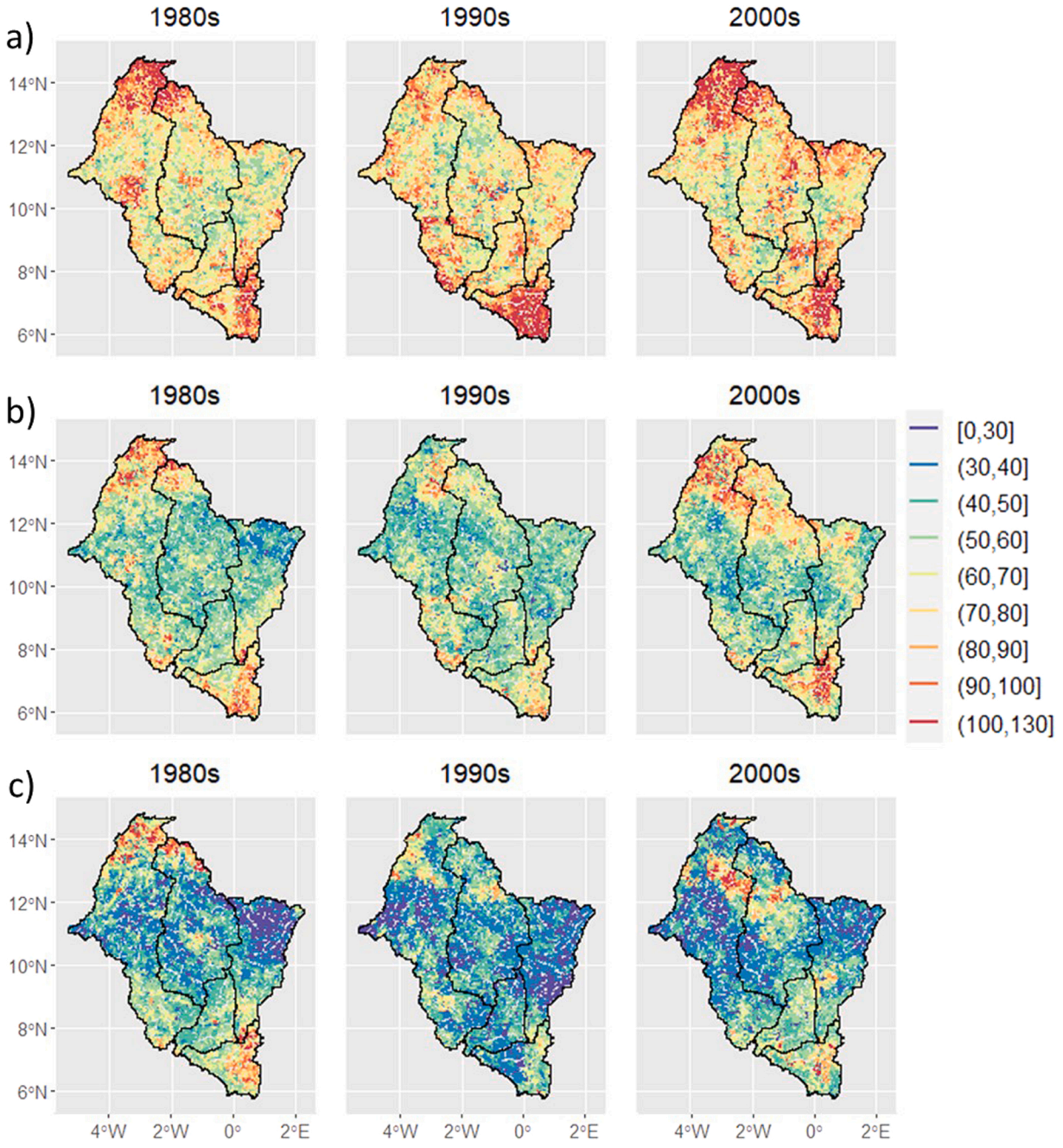

Fig. 9. Drought duration (days) in moderate (a), severe (b), and extreme (c) droughts averaged over the period 1980–1990 (1980 s), 1991–2000 (1990 s), and 2001–2010 (2000 s). Black lines are catchment boundaries.

severe droughts, whilst extreme droughts have become longer and more severe in the northeast.

In reality, the trends in many areas will likely be impacted by the presence and operation of upstream dams, for which there tends to be a higher observed drought duration and severity compared to the modeled data.

3.4. Decadal variability in drought duration and severity

Even though there are increasing and decreasing trends in drought duration and severity, there is high decadal variability across the time period. To assess this variability, we calculated the drought statistics over three decades: 1981–1990 (1980 s), 1991–2000

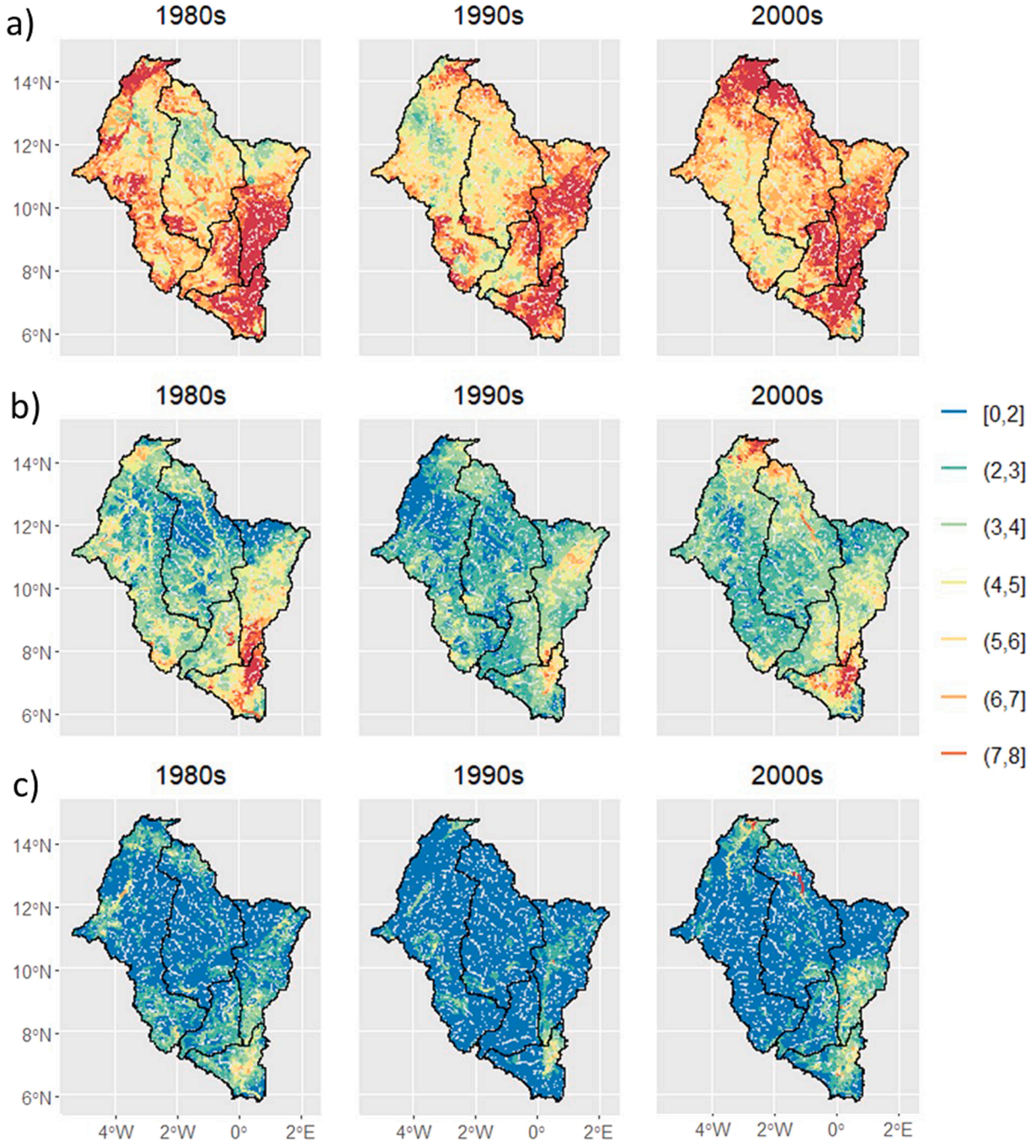

Fig. 10. Normalised drought severity (m^3s^{-1} / m^3s^{-1}) of moderate (a), severe (b), and extreme (c) droughts averaged over the periods 1981–1990 (1980 s), 1991–2000 (1990 s), and 2001–2010 (2000 s). Black lines are catchment boundaries.

(1990 s), and 2001–2010 (2000 s). The result shows large differences in drought duration and severity between the three decades, with spatial variability in the drought characteristics in different decades (Figs. 9 and 10). Moderate drought duration is higher during the 1980 s and 2000 s in northern Volta compared to the 1990 s (Fig. 9). The White Volta shows an increasing tendency from the 1980–2000 s, and the Black and Lower Volta basins show high variability between the three decades. The maximum number of moderate droughts (100–130 days) is observed in southern and northern Volta during each decade. Similar to moderate droughts, severe droughts show a high number of drought durations in the north and south part of Volta, with a reduction during the 1990 s and a maximum of up to 100–130 days in the other decades. The duration of extreme droughts is also lower in the 1990 s, particularly in the Lower Volta, Oti River and White Volta.

The normalised severity similarly shows spatial and temporal variability across the three time periods (Fig. 10). Moderate drought severity is higher in the Black Volta, Lower Volta and Oti compared to the White Volta in the 1980 s. However, moderate drought severity in the Black Volta is lower during the 1990 s and 2000 s. The Oti River and Lower Volta show a higher severity in all periods. In the 1990 s, the severity for severe and extreme droughts is lower in a large part of the Volta compared to the 1980 s and 2000 s. In general, the Oti River and Lower Volta showed a higher severity in all periods compared to the White Volta.

3.5. *Streamflow-precipitation relationship and drought propagation*

The correlation with streamflow increases from 1- to 30-days and decreases thereafter. The correlation varies depending on the climate and upstream catchment area. In wetter and larger catchments (9000–16000 km^2), the correlation is very high (from 0.74 to 0.84) compared to drier and smaller catchments (130–4500), with correlations from 0.65 to 0.71 for 30-day antecedent precipitation (Fig. 11a). An example is provided in Fig. 11a for 12 river reaches selected from White Volta, Black Volta, Oti River, and Lower Volta, which shows that the highest correlation is for a 30-days average. The location of the 12 river reachs (River ID) is provided in the suplimentary material (SFig. 1). Moreover, there is a clear propagation from meteorological drought to hydrological drought. Using the same threshold level for the 30-day average precipitation, on average the propagation to streamflow droughts start two weeks after the start of the meteorological drought (Fig. 11b), but this varies depending on the season (wet versus dry) and length of the meteorological drought. Fig. 11b also shows negative lag values indicating streamflow drought starts before meteorological droughts. Longer meteorological droughts increase the duration and severity of streamflow droughts. During wetter months, streamflow droughts can start up to a month after meteorological droughts. During dry months, however, the lag is much smaller with hydrological droughts starting quickly (1 – 10 days) after meteorological droughts.

4. Discussion

4.1. *Uncertainties in the modeled streamflow*

One of the main challenges in assessing and understanding drought in the region is the limited availability of high-quality,

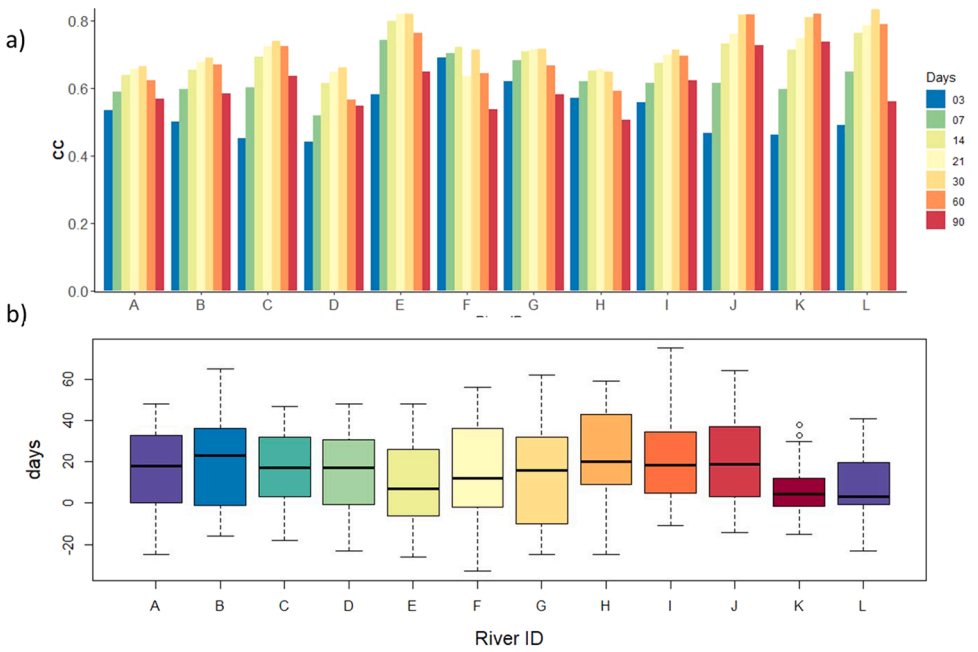

Fig. 11. (a) Temporal correlation of daily streamflow and 3, 7, 14, 21, 30, 60, and 90 days average precipitation, and (b) propagation of meteorological to hydrological droughts for moderate drought (Q70) and for selected river reaches (River ID) from Black, White, Oti and Lower Volta.

measured hydro-climate data to allow long-term analysis and especially across different scales down to the catchment level (van Huijgevoort et al., 2013). Hydrological models driven by the most accurate meteorological forcing, developed from a combination of remote sensing, climate model and observations, are a plausible alternative to represent regional terrestrial water cycles for drought analysis (van Huijgevoort et al., 2013). Here we used reliable and widely used meteorological forcing datasets available at a high spatial and temporal resolution and for multiple decades to drive a widely applied and tested hydrological model. Nevertheless, there are several uncertainties in the modelling approach, which affect the results and their interpretation.

Hydrological droughts are strongly modified by natural conditions such as land cover and soil type, as well as human activities such as changes in land use, storage and redistribution of water, which influence the propagation of precipitation through the hydrological system and modify drought characteristics (Van Loon et al., 2016). In the Volta basin, the increase in water storage and abstraction by riparian countries to meet demand has driven water stress, streamflow droughts and competition over water resources (van de Giesen et al., 2001; Mul et al., 2015). These management activities, including the numerous dams and associated reservoirs across the basin, which show a DOR of between 0.1% and 500%, are not represented in the version of the VIC model used here. Therefore, the skill of the model in representing actual streamflow, particularly in major rivers of the White, Black, Oti, and Lower Volta (Fig. 1), is affected by the presence of these hydraulic structures and their impact on streamflow. Nevertheless, the model captures the overall variability and does reasonably well in representing the characteristics of hydrological drought at stations with adequate observed data records and with fewer upstream dams. Taking one of the stations, Nawuni (catchment area = 93,000 km^2), with the longest record, a low number of data gaps, and a large number of upstream dams and reservoirs (DOR=40%), the daily and monthly correlation is higher than 90% and the mean duration for moderate, severe, and extreme droughts shows an average under-estimation of about 20 days. Given the mean drought duration of about 40–60 days from the model, this under-estimation is significant and is likely influenced by the lack of representation in the model of upstream water abstraction and water holding by the dams. In basins with significant human impacts, it is therefore not possible to model drought events with confidence, and a new framework is required to assess droughts that takes into account (often unknown) dam operations and water abstraction (Van Loon et al., 2016).

The input climate data, particularly precipitation, provide additional uncertainties. Although there have been no specific evaluations of MSWEP for the Volta basin that we are aware of, it is likely suitable for this application given evaluations for other regions and globally. Several studies have evaluated MSWEP in terms of its reliability as compared to station data and against other gridded datasets, but also in how well streamflow observations are simulated when used to force a hydrological model, which is of interest here. MSWEP captures extreme events in different climate regions and generates streamflow data (including high and low flows) with higher accuracy compared to other satellite-based precipitation datasets (Tang et al., 2019) and provides the highest daily correlation globally (Beck et al., 2016). In addition, MSWEP was found to produce reliable streamflow in the Nile basin in Ethiopia (Lakew, 2020) and globally (Lin et al., 2019). Furthermore, VIC has a large number of parameters, with the most sensitive ones for runoff generation, such as the infiltration curve and soil thickness parameters, which are somewhat constrained by calibration to the overall streamflow regime, but not necessarily to the low flows. These may be driven by groundwater sources, which are not well represented in the model. Additional uncertainties in other parameters will contribute to the overall uncertainties.

4.2. *Spatial distribution and propagation of drought*

The results show diversity in drought characteristics across the basin. Drought duration days are higher in the north for all threshold levels, which reflects the north-south climate gradient, with streamflow conditions persisting in relatively drier states for longer in the drier conditions of the north. The variability in severity is mainly due to the size of the catchment but will also be influenced by the temporal variability in precipitation which is lower in the north and higher in the south. Drought duration varies from place to place due to many local factors such as air temperature, precipitation, soil type, topography, and antecedent conditions that will determine the persistence of anomalies in precipitation as they propagate through the hydrological system. In particular, differences in the temporal variability of precipitation across the basin will drive differences in drought duration (Sheffield et al., 2004) with low variability in the drier north leading to longer droughts, and vice-versa in the wetter, more variable south. The differences in seasonal variability in precipitation may also play a role with the distinct dry season in the north potentially influencing drought duration by extending drought conditions that emerge in the wet season. In the south, the year round precipitation provides an opportunity to recover droughts that emerge in the wetter part of the year. The hotspot of longer droughts and maximum severity in the southeast may be related to the observed increase in dry spell days and decreasing trend in precipitation extremes, such as heavy and very heavy rainfall days (Klassou and Komi, 2021). The distribution of severity is more complex and depends on how it is normalized, but generally follows the pattern of drought duration when normalized by MAF, and a northwest to southeast gradient when normalized by area.

We assessed the relationship between precipitation and streamflow by identifying the time scale of antecedent precipitation (from 1 to 90 days mean) that correlated most strongly with streamflow for all river reaches and found the highest correlation for the 30-day mean. For streamflow drought, in particular, we found a clear propagation from meteorological to hydrological drought with an average lag-time of two weeks although with large variation (1–45 days) depending on the climate (wet or dry) and upstream catchment size. In general, there is a strong relationship between meteorological and hydrological droughts in arid and semi-arid areas (Peters et al., 2006; Vidal et al., 2010; Van Loon and Laaha, 2015) with lag times similar to this study. The relationship shown here for the Volta is weaker in smaller and drier catchments, which indicates the additional complexity of the propagation that may also be seasonally dependent. Other catchment characteristics (e.g., elevation, soil type, geology and land cover) and processes modulate the partitioning of precipitation into evapotranspiration and runoff, and the translation into streamflow, and importantly in the context of drought, the generation of subsurface flows that can maintain streamflow during meteorological drought (Chiverton et al., 2015;

Tijdeman et al., 2018; van Oel et al., 2018; Van Tiel et al., 2021). This includes the dynamics of soil-water content and groundwater storage (Hughes, 1998) that are influenced by soil and aquifer characteristics, and the connection to the stream network. Groundwater droughts will have a longer lag time (e.g. 45 days, Li et al., 2018) caused by the delay in recharge and residence time in the aquifer.

4.3. Drivers of changes in streamflow drought

We found high temporal variability in drought duration and severity across the Volta basin during 1979–2013. The maximum severity occurred in the 1980 s, which is in line with known climate variability and the decrease in precipitation in the 1970–1980 s. The 1980 s were the driest decade in West Africa compared to the period of 1901–1970 (Nicholson and Palao, 1993) and more than 90 % of the basin faced extreme metrological drought (van de Giesen et al., 2010; Kasei et al., 2009), which led to food insecurity for more than 50% of the population (Kasei et al., 2009).

Studies have indicated that the droughts in the Sahel region in the 1970 s and 1980 s were influenced by anthropogenic warming, which caused a shift in sea surface temperatures (SST) in the Indo-Pacific oceans and tropical Atlantic (Park et al., 2016). For example, SST-based indices such as ENSO, Atlantic Niño, and Tropical Indian Ocean (TIO), tend to show the largest connection to the variability in streamflow extremes across West Africa (Chun et al., 2021). In addition, increasing SSTs in the Gulf of Guinea and South Atlantic Ocean have been associated with droughts, which is a common feature in the tropics (Rowell et al., 1995; Hoerling et al., 2006). A clear link between droughts and Indian Ocean warming has also been shown for the region over the period 1950–1990 (Hoerling et al., 2006) and this is expected to lead to increased droughts in the 21st century with warming of the Indian Ocean.

4.4. Implications and Future Changes

Overall, the model data show an increasing trend in streamflow drought in the Lower Volta, and a decreasing trend in the northeastern part of the basin, which is in part a rebound from the dry conditions of the 1980 s (Trenberth et al., 2007). In the Volta and West Africa in general, the amount and duration of daily precipitation has declined since the 1970 s and led to an increase in moderate and severe drought durations (Kasei et al., 2009; Oguntunde et al., 2017; Owusu et al., 2008). Future climate projections for the Volta Basin indicate an increase in the magnitude and frequency of droughts (Oguntunde et al., 2020). This will further impact water availability for agriculture, energy and other public needs, and will be aggravated by the projected increase in population and related demand for water for agriculture, energy and food production (IPCC, 2013). In the Volta basin, more than 90% of the agricultural land is rainfed and managed by smallholder farmers (Kasei et al., 2009), which makes it more susceptible to the projected change and variability in climate.

5. Summary and conclusion

Droughts are one of the main challenges in Africa affecting the agriculture and energy sectors, and livelihoods of millions of Africans, particularly those in rural areas which mainly depend on rain-fed agriculture. Due to its natural complexity, however, it is very difficult to manage, monitor and mitigate drought and its impacts. The impact of droughts is exacerbated due to the lack of water storage infrastructure and limited knowledge and up to date information on their changes and variability and links to climate drivers. As a basis to effectively manage and monitor droughts at a basin and sub-catchment level, we provided a detailed analysis of variability and changes in droughts based on streamflow data simulated using the VIC and RAPID modelling system for 10,300 river reaches. The application of a high-resolution hydrological modelling framework has allowed the assessment of changes and variability in drought duration and severity at a much finer scale than previous studies in the region, which helps to identify hotspot areas of drought hazard, which can inform the development of adaptation measures accordingly.

Based on the simulated flow, drought duration days and severity showed high variability in space and time through the three decades of analysis. The number of drought duration days are higher in the north and south and lower in central parts of the basin. The Oti River and Northern Volta show the highest severity, compared to the Black, White, and Lower Volta. Drought duration and severity was generally higher in the 1980 s. Drought duration and severity generally decreases in the north and northeastern parts of the basin since the 1980 s and increased in the lower part. The observed increase in the south (up to 2.5% per event) and decrease (up to 5% per event) in the north in drought duration days might not cause a significant impact on the agriculture, water supply and energy sectors. However, the change in severity, which is up to − 20% per event in the Lower Volta, might cause an impact on the hydroelectric (e.g., Akosombo dam) and irrigation dams. On the other hand, existing and planned irrigation and multipurpose dams in the upper part of the Black and the north part Volta, in general, will benefit from the decrease in severity as a result of the increase in precipitation. In general, considering the importance of the basin for water supply, irrigation and energy for the six countries that share the basin, these changes have implications for how water resources are managed in the basin, including the need for early warning strategies to reduce the environmental and socio-economic impacts of drought.

CRediT authorship contribution statement

Solomon Gebrechorkos: Conceptualization, Methodology, Formal analysis, and writing. **Ming Pan:** Software, Validation. **Peirong Lin:** Software, Validation. **Daniela Anghileri:** Formal analysis, Validation. **Nathan Forsythe:** Formal analysis, Resources. **David Pritchard:** Formal analysis, Resources. **Hayley Fowler:** Writing – review & editing. **Emmanuel Obuobie:** Formal analysis, Resources. **Deborah Darko:** Formal analysis, Resources. **Justin Sheffield:** Conceptualization, Writing –review & editing, Supervision.

Declaration of Competing Interest

The authors declare that they have no known competing financial interests or personal relationships that could have appeared to influence the work reported in this paper.

Data Availability

The Princeton Global Forcings (PGF) (Sheffield et al., 2006) is freely available at Princeton University, Terrestrial hydrology (http://hydrology.princeton.edu/data.pgf.php) and the Multi-Source Weighted-Ensemble Precipitation (MSWEP, Beck et al., 2016) is available at the GloH2O (http://www.gloh2o.org/mswep/).

Acknowledgements

This work was supported by the “FutureDams: Design and Assessment of water-energy-food-environment Mega Systems” project [ES/P011373/1] and the ‘Building REsearch Capacity for Sustainable Water and Food Security In drylands of Sub-Saharan Africa’ (BRECcIA) project [NE/P021093/1], which are supported by UK Research and Innovation as part of the Global Challenges Research Fund.

Appendix A. Supporting information

Supplementary data associated with this article can be found in the online version at doi:10.1016/j.ejrh.2022.101143.

References

Figures.
AghaKouchak, A., Cheng, L., Mazdiyasni, O., Farahmand, A., 2014. Global warming and changes in risk of concurrent climate extremes: Insights from the 2014 California drought. Geophys. Res. Lett. 41, 8847–8852. https://doi.org/10.1002/2014GL062308.
Ayana, E.K., Ceccato, P., Fisher, J.R.B., DeFries, R., 2016. Examining the relationship between environmental factors and conflict in pastoralist areas of East Africa. Sci. Total Environ. 557–558, 601–611. https://doi.org/10.1016/j.scitotenv.2016.03.102.
B. Barry, B., Obuobie, E., Andreini, M., Andah, W., Pluquet, M., 2005. The Volta river basin. Comparative study of river basin development and management Rapp., IWMI, CAWMA.
Ballarin, A.S., Barros, G.L., Cabrera, M.C.M., Wendland, E.C., 2021. A copula-based drought assessment framework considering global simulation models. J. Hydrol.: Reg. Stud. 38, 100970 https://doi.org/10.1016/j.ejrh.2021.100970.
Barkstrom, B.R., Harrison, E.F., Smith, G.L., Cess, R.D., 1989. Results from the Earth Radiation Budget Experiment (ERBE). Adv. Space Res. 9, 75–82. https://doi.org/10.1016/0273-1177(89)90146-4.
Bates, B.C., Kundzewicz, Z.W., Wu, S., Palutikof, J.P., 2008. Climate Change and Water (Technical Paper of the Intergovernmental Panel on Climate Change). IPCC Secretariat, Geneva, Switzerland.
Beck, H.E., de Roo, A., van Dijk, A.I.J.M., 2015. Global Maps of Streamflow Characteristics Based on Observations from Several Thousand Catchments. J. Hydrometeorol. 16, 1478–1501. https://doi.org/10.1175/JHM-D-14-0155.1.
Beck, H.E., van Dijk, A.I.J.M., Levizzani, V., Schellekens, J., Miralles, D.G., Martens, B., de Roo, A., 2016. MSWEP: 3-hourly 0.25°global gridded precipitation (1979-2015) by merging gauge, satellite, and reanalysis data. Hydrol. Earth Syst. Sci. Discuss. 1–38. https://doi.org/10.5194/hess-2016-236.
Beck, H.E., Vergopolan, N., Pan, M., Levizzani, V., Dijk, A.I.J.M., van, Weedon, G.P., Brocca, L., Pappenberger, F., Huffman, G.J., Wood, E.F., 2017. Global-scale evaluation of 22 precipitation datasets using gauge observations and hydrological modeling. Hydrol. Earth Syst. Sci. 21, 6201–6217. https://doi.org/10.5194/hess-21-6201-2017.
Beck, H.E., Wood, E.F., Pan, M., Fisher, C.K., Miralles, D.G., van Dijk, A.I.J.M., McVicar, T.R., Adler, R.F., 2018. MSWEP V2 global 3-hourly 0.1° precipitation: methodology and quantitative assessment. Bull. Am. Meteor. Soc. 100, 473–500. https://doi.org/10.1175/BAMS-D-17-0138.1.
Beyene, B.S., Van Loon, A.F., Van Lanen, H. a J., Torfs, P.J.J.F., 2014. Investigation of variable threshold level approaches for hydrological drought identification. Hydrol. Earth Syst. Sci. Discuss. 11, 12765–12797. https://doi.org/10.5194/hessd-11-12765-2014.
Chen, L., Dirmeyer, P.A., 2016. Impacts of land-use/land-cover change on afternoon precipitation over North America. J. Clim. 30, 2121–2140. https://doi.org/10.1175/JCLI-D-16-0589.1.
Chen, L., Dirmeyer, P.A., Tawfik, A., Lawrence, D.M., 2017. Sensitivities of land cover–precipitation feedback to convective triggering. J. Hydrometeorol. 18, 2265–2283. https://doi.org/10.1175/JHM-D-17-0011.1.
Chiverton, A., Hannaford, J., Holman, I., Corstanje, R., Prudhomme, C., Bloomfield, J., Hess, T.M., 2015. Which catchment characteristics control the temporal dependence structure of daily river flows. Hydrol. Process. 29, 1353–1369. https://doi.org/10.1002/hyp.10252.

Chun, K.P., Dieppois, B., He, Q., Sidibe, M., Eden, J., Paturel, J.-E., Mahé, G., Rouché, N., Klaus, J., Conway, D., 2021. Identifying drivers of streamflow extremes in West Africa to inform a nonstationary prediction model. Weather Clim. Extrem. 33, 100346 https://doi.org/10.1016/j.wace.2021.100346.
Unisdr Cred, 2015. The human cost of natural disasters: a global perspective.
CRED, 2018. Economic losses, poverty & disasters: 1998–2017.
Dai, A., 2013. Increasing drought under global warming in observations and models. Nat. Clim. Change 3, 52–58. https://doi.org/10.1038/nclimate1633.
Dang, T.D., Vu, D.T., Chowdhury, A.F.M.K., Galelli, S., 2020. A software package for the representation and optimization of water reservoir operations in the VIC hydrologic model. Environ. Model. Softw. 126, 104673 https://doi.org/10.1016/j.envsoft.2020.104673.
David, C.H., Maidment, D.R., Niu, G.-Y., Yang, Z.-L., Habets, F., Eijkhout, V., 2011. River network routing on the NHDPlus dataset. J. Hydrometeorol. 12, 913–934. https://doi.org/10.1175/2011JHM1345.1.
Demaria, E.M.C., Maurer, E.P., Sheffield, J., Bustos, E., Poblete, D., Vicuña, S., Meza, F., 2012. Using a gridded global dataset to characterize regional hydroclimate in central Chile. J. Hydrometeorol. 14, 251–265. https://doi.org/10.1175/JHM-D-12-047.1.
Dierauer, J., Whitfield, P., 2019. Daily Streamflow Trend and Change Point Screening.
Ferreira, V.G., Andam-Akorful, S.A., Dannouf, R., Adu-Afari, E., 2019. A Multi-Sourced Data Retrodiction of Remotely Sensed Terrestrial Water Storage Changes for West Africa. Water 11, 401. https://doi.org/10.3390/w11020401.
Fleig, A.K., Tallaksen, L.M., Hisdal, H., Demuth, S., 2006. A global evaluation of streamflow drought characteristics. Hydrol. Earth Syst. Sci. 10, 535–552. https://doi.org/10.5194/hess-10-535-2006.
Gebrechorkos, S.H., Hülsmann, S., Bernhofer, C., 2018. Evaluation of multiple climate data sources for managing environmental resources in East Africa. Hydrol. Earth Syst. Sci. 22, 4547–4564. https://doi.org/10.5194/hess-22-4547-2018.
Gebrechorkos, S.H., Hülsmann, S., Bernhofer, C., 2019. Regional climate projections for impact assessment studies in East Africa. Environ. Res. Lett. 14, 044031 https://doi.org/10.1088/1748-9326/ab055a.
Gebrechorkos, S.H., Bernhofer, C., Hülsmann, S., 2020. Climate change impact assessment on the hydrology of a large river basin in Ethiopia using a local-scale climate modelling approach. Sci. Total Environ. 742, 140504 https://doi.org/10.1016/j.scitotenv.2020.140504.
Giesen, N. van de, Andreini, M.S., Edig, A. van, Vlek, P.L.G., 2001. Competition for water resources of the Volta basin.
Gordon, C., Nukpeza, D., Tweneboah-Lawson, E., Ofori, B., Yirenya-Taiwiah, D.R., Ayivor, J.S., Koranteng, S., Darko, D., Mensah, A., 2013. West Africa – water resources vulnerability using a multidimensional approach: case study of volta basin. Clim. Vulnerability: Underst. Address Threats Essent. Resour. https://doi.org/10.1016/B978-0-12-384703-4.00518-9.
GRDC, 2019. The Global Runoff Data Centre, 56068 Koblenz, Germany [WWW Document]. URL ⟨https://www.bafg.de/GRDC/EN/02_srvcs/21_tmsrs/riverdischarge_node.html⟩.
Haile, G.G., Tang, Q., Leng, G., Jia, G., Wang, J., Cai, D., Sun, S., Baniya, B., Zhang, Q., 2020. Long-term spatiotemporal variation of drought patterns over the Greater Horn of Africa. Sci. Total Environ. 704, 135299 https://doi.org/10.1016/j.scitotenv.2019.135299.
Hoerling, M., Hurrell, J., Eischeid, J., Phillips, A., 2006. Detection and attribution of twentieth-century Northern and Southern African rainfall change. J. Clim. 19, 3989–4008. https://doi.org/10.1175/JCLI3842.1.
Hughes, D.A., 1998. Antecedent Precipitation, in: Encyclopedia of Hydrology and Lakes, Encyclopedia of Earth Science, 69–69. Springer, Netherlands, Dordrecht. https://doi.org/10.1007/1-4020-4497-6_16.
IPCC, 2012. Managing the Risks of Extreme Events and Disasters to Advance Climate Change Adaptation. URL ⟨https://www.ipcc.ch/report/managing-the-risks-of-extreme-events-and-disasters-to-advance-climate-change-adaptation/⟩ (accessed 5.13.20).
IPCC, 2013. Climate Change 2013: The Physical Science Basis. In: Stocker, et al. (Eds.), (WG1). Cambridge Univ Press.
Jones, S.K., Fremier, A.K., DeClerck, F.A., Smedley, D., Ortega Pieck, A., Mulligan, M., 2017. Big data and multiple methods for mapping small reservoirs: comparing accuracies for applications in agricultural landscapes. Remote Sens. 9, 1307. https://doi.org/10.3390/rs9121307.
Kasei, R., Diekkrüger, B., Leemhuis, C., 2009. Drought frequency in the Volta Basin of West Africa. Sustain. Sci. 5, 89. https://doi.org/10.1007/s11625-009-0101-5.
Kendall, M., 1975. Rank Correlation Measures.
Klassou, K.S., Komi, K., 2021. Analysis of extreme rainfall in Oti River Basin (West Africa). J. Water Clim. Change 12, 1997–2009. https://doi.org/10.2166/wcc.2021.154.
Lakew, H.B., 2020. Investigating the effectiveness of bias correction and merging MSWEP with gauged rainfall for the hydrological simulation of the upper Blue Nile basin. J. Hydrol.: Reg. Stud. 32, 100741 https://doi.org/10.1016/j.ejrh.2020.100741.
Lehner, B., Liermann, C.R., Revenga, C., Vörösmarty, C., Fekete, B., Crouzet, P., Döll, P., Endejan, M., Frenken, K., Magome, J., Nilsson, C., Robertson, J.C., Rödel, R., Sindorf, N., Wisser, D., 2011. High-resolution mapping of the world's reservoirs and dams for sustainable river-flow management. Front. Ecol. Environ. 9, 494–502. https://doi.org/10.1890/100125.
Leonard, M., Westra, S., Phatak, A., Lambert, M., van den Hurk, B., McInnes, K., Risbey, J., Schuster, S., Jakob, D., Stafford-Smith, M., 2014. A compound event framework for understanding extreme impacts. WIREs Clim. Change 5, 113–128. https://doi.org/10.1002/wcc.252.
Liang, X., Lettenmaier, D.P., Wood, E.F., Burges, S.J., 1994. A simple hydrologically based model of land surface water and energy fluxes for general circulation models. J. Geophys. Res.: Atmos. 99, 14415–14428. https://doi.org/10.1029/94JD00483.
Lin, P., Pan, M., Beck, H.E., Yang, Y., Yamazaki, D., Frasson, R., David, C.H., Durand, M., Pavelsky, T.M., Allen, G.H., Gleason, C.J., Wood, E.F., 2019. Global reconstruction of naturalized river flows at 2.94 million reaches. Water Resour. Res. 55, 6499–6516. https://doi.org/10.1029/2019WR025287.
Liu, Q., McVicar, T.R., Yang, Z., Donohue, R.J., Liang, L., Yang, Y., 2016. The hydrological effects of varying vegetation characteristics in a temperate water-limited basin: development of the dynamic Budyko-Choudhury-Porporato (dBCP) model. J. Hydrol. 543, 595–611. https://doi.org/10.1016/j.jhydrol.2016.10.035.
Lyon, B., DeWitt, D.G., 2012. A recent and abrupt decline in the East African long rains. Geophys. Res. Lett. 39, L02702. https://doi.org/10.1029/2011GL050337.
Martens, B., Miralles, D.G., Lievens, H., Schalie, R., van der, Jeu, R.A.M., de, Fernández-Prieto, D., Beck, H.E., Dorigo, W.A., Verhoest, N.E.C., 2017. GLEAM v3: satellite-based land evaporation and root-zone soil moisture. Geosci. Model Dev. 10, 1903–1925. https://doi.org/10.5194/gmd-10-1903-2017.
Masih, I., Maskey, S., Mussá, F.E.F., Trambauer, P., 2014. A review of droughts on the African continent: a geospatial and long-term perspective. Hydrol. Earth Syst. Sci. 18, 3635–3649. https://doi.org/10.5194/hess-18-3635-2014.
Mccartney, M.P., Forkuor, G., Sood, A., Amisigo, B., Hattermann, F., Muthuwatta, L.P., 2012. The water resource implications of changing climate in the Volta River Basin [Africa]. https://doi.org/10.5337/2012.219.
McDowell, G., Ford, J., Jones, J., 2016. Community-level climate change vulnerability research: trends, progress, and future directions. Environ. Res. Lett. 11, 033001 https://doi.org/10.1088/1748-9326/11/3/033001.
McKee, T.B., Doesken, N.J., Kliest, J., 1993. The relationship of drought frequency and duration to time scales. In Proceedings of the 8th Conference of Applied Climatology, 17–22 January, Anaheim, CA. American Meterological Society, Boston, MA. pp. 179–184.
Melsen, L.A., Guse, B., 2019. Hydrological drought simulations: how climate and model structure control parameter sensitivity. Water Resour. Res. 55, 10527–10547. https://doi.org/10.1029/2019WR025230.
Mishra, A.K., Singh, V.P., 2010. A review of drought concepts. J. Hydrol. 391, 202–216. https://doi.org/10.1016/j.jhydrol.2010.07.012.
Mukherjee, S., Mishra, A., Trenberth, K.E., 2018. Climate change and drought: a perspective on drought indices. Curr. Clim. Change Rep. 4, 145–163. https://doi.org/10.1007/s40641-018-0098-x.

Mul, M., Obuobie, E., Appoh, R., Kankam-Yeboah, K., Bekoe-Obeng, E., Amisigo, B., Logah, F.Y., Ghansah, B., McCartney, M., 2015. Water resources assessment of the Volta River Basin. International Water Management Institute (IWMI). https://doi.org/10.5337/2015.220.

Naumann, G., Alfieri, L., Wyser, K., Mentaschi, L., Betts, R.A., Carrao, H., Spinoni, J., Vogt, J., Feyen, L., 2018. Global changes in drought conditions under different levels of warming. Geophys. Res. Lett. 45, 3285–3296. https://doi.org/10.1002/2017GL076521.

New, M., Hulme, M., Jones, P., 1999. Representing twentieth-century space–time climate variability. Part I: development of a 1961–90 mean monthly terrestrial climatology. J. Clim. 12, 829–856. https://doi.org/10.1175/1520-0442(1999)012<0829:RTCSTC>2.0.CO;2.

New, M., Hulme, M., Jones, P., 2000. Representing twentieth-century Space–time climate variability. Part II: development of 1901–96 monthly grids of terrestrial surface climate. J. Clim. 13, 2217–2238. https://doi.org/10.1175/1520-0442(2000)013<2217:RTCSTC>2.0.CO;2.

Ngcamu, B.S., Chari, F., 2020. Drought influences on food insecurity in Africa: a systematic literature review. Int. J. Environ. Res. Public Health 17, 5897. https://doi.org/10.3390/ijerph17165897.

Niang, I., Ruppel, O.C., Abdrabo, M.A., Essel, A., Lennard, C., Padgham, J., Urquhart, P., 2014. WG2. In: Barros, V.R., et al. (Eds.), Africa. In: Climate Change 2014: Impacts, Adaptation, and Vulnerability. Part B: Regional Aspects. Cambridge Univ. Press.

Nicholson, S.E., 2017. Climate and climatic variability of rainfall over eastern Africa. Rev. Geophys. 55, 590–635. https://doi.org/10.1002/2016RG000544.

Nicholson, S.E., Palao, I.M., 1993. A re-evaluation of rainfall variability in the sahel. Part I. Characteristics of rainfall fluctuations. Int. J. Climatol. 13, 371–389. https://doi.org/10.1002/joc.3370130403.

Oguntunde, P.G., Abiodun, B.J., Lischeid, G., 2017. Impacts of climate change on hydro-meteorological drought over the Volta Basin, West Africa. Glob. Planet. Change 155, 121–132. https://doi.org/10.1016/j.gloplacha.2017.07.003.

Oguntunde, P.G., Abiodun, B.J., Lischeid, G., Abatan, A.A., 2020. Droughts projection over the Niger and Volta River basins of West Africa at specific global warming levels. Int. J. Climatol. 40, 5688–5699. https://doi.org/10.1002/joc.6544.

Oloruntade, A.J., Mohammad, T.A., Ghazali, A.H., Wayayok, A., 2017. Analysis of meteorological and hydrological droughts in the Niger-South Basin, Nigeria. Glob. Planet. Change 155, 225–233. https://doi.org/10.1016/j.gloplacha.2017.05.002.

Owusu, K., Waylen, P., Qiu, Y., 2008. Changing rainfall inputs in the Volta basin: implications for water sharing in Ghana. GeoJournal 71, 201–210. https://doi.org/10.1007/s10708-008-9156-6.

Park, J., Bader, J., Matei, D., 2016. Anthropogenic Mediterranean warming essential driver for present and future Sahel rainfall. Nat. Clim. Change 6, 941–945. https://doi.org/10.1038/nclimate3065.

Peters, E., Bier, G., van Lanen, H.A.J., Torfs, P.J.J.F., 2006. Propagation and spatial distribution of drought in a groundwater catchment. J. Hydrol. 321, 257–275. https://doi.org/10.1016/j.jhydrol.2005.08.004.

Rivera, J.A., Araneo, D.C., Penalba, O.C., 2017. Threshold level approach for streamflow drought analysis in the Central Andes of Argentina: a climatological assessment. Hydrol. Sci. J. 62, 1949–1964. https://doi.org/10.1080/02626667.2017.1367095.

Rivera, J.A., Araneo, D.C., Penalba, O.C., Villalba, R., 2018. Regional aspects of streamflow droughts in the Andean rivers of Patagonia, Argentina. Links with large-scale climatic oscillations. Hydrol. Res. 49, 134–149. https://doi.org/10.2166/nh.2017.207.

Rodgers, C., van de Giesen, N., Laube, W., Vlek, P.L.G., Youkhana, E., 2007. The GLOWA Volta Project: A framework for water resources decision-making and scientific capacity building in a transnational West African basin. In: Craswell, E., Bonnell, M., Bossio, D., Demuth, S., Van De Giesen, N. (Eds.), Integrated Assessment of Water Resources and Global Change: A North-South Analysis. Springer, Netherlands, Dordrecht, pp. 295–313. https://doi.org/10.1007/978-1-4020-5591-1_18.

Rowell, D.P., Folland, C.K., Maskell, K., Ward, M.N., 1995. Variability of summer rainfall over tropical north Africa (1906–92): observations and modelling. Q. J. R. Meteorol. Soc. 121, 669–704. https://doi.org/10.1002/qj.49712152311.

Schellekens, J., Dutra, E., Martínez-de la Torre, A., Balsamo, G., Dijk, A. van, Sperna, Weiland, Minvielle, F., Calvet, M., Decharme, J.-C., Eisner, B., Fink, S., Flörke, G., Peßenteiner, M., Beek, S., van, R., Polcher, J., Beck, H., Orth, R., Calton, B., Burke, S., Dorigo, W., Weedon, G.P., 2017. A global water resources ensemble of hydrological models: the eartH2Observe Tier-1 dataset. Earth System Science Data 389–413. https://doi.org/10.5194/essd-9-389-2017.

Sen, P.K., 1968. Estimates of the regression coefficient based on Kendall's Tau. J. Am. Stat. Assoc. 63, 1379–1389. https://doi.org/10.1080/01621459.1968.10480934.

Sheffield, J., Wood, E.F., 2008. Projected changes in drought occurrence under future global warming from multi-model, multi-scenario, IPCC AR4 simulations. Clim. Dyn. 31, 79–105. https://doi.org/10.1007/s00382-007-0340-z.

Sheffield, J., Goteti, G., Wen, F., Wood, E.F., 2004. A simulated soil moisture based drought analysis for the United States. J. Geophys. Res.: Atmos. 109. https://doi.org/10.1029/2004JD005182.

Sheffield, J., Goteti, G., Wood, E.F., 2006. Development of a 50-Year high-resolution global dataset of meteorological forcings for land surface modeling. J. Clim. 19, 3088–3111. https://doi.org/10.1175/JCLI3790.1.

Sheffield, J., Wood, E.F., Roderick, M.L., 2012. Little change in global drought over the past 60 years. Nature 491, 435–438. https://doi.org/10.1038/nature11575.

Shukla, S., Wood, A.W., 2008. Use of a standardized runoff index for characterizing hydrologic drought. Geophys. Res. Lett. 35. https://doi.org/10.1029/2007GL032487.

Sivakumar, M.V.K., Stefanski, R., Bazza, M., Zelaya, S., Wilhite, D., Magalhaes, A.R., 2014. High Level Meeting on National Drought Policy: Summary and Major Outcomes. Weather Clim. Extremes 3, 126–132. https://doi.org/10.1016/j.wace.2014.03.007.

Stanke, C., Kerac, M., Prudhomme, C., Medlock, J., Murray, V., 2013. Health effects of drought: a systematic review of the evidence. PLoS Curr. 5. https://doi.org/10.1371/currents.dis.7a2cee9e980f91ad7697b570bcc4b004.

Sternberg, T., 2011. Regional drought has a global impact, 169–169 Nature 472. https://doi.org/10.1038/472169d.

Tang, X., Zhang, J., Gao, C., Ruben, G.B., Wang, G., 2019. Assessing the uncertainties of four precipitation products for swat modeling in Mekong river basin. Remote Sens. 11, 304. https://doi.org/10.3390/rs11030304.

Tijdeman, E., Hannaford, J., Stahl, K., 2018. Human influences on streamflow drought characteristics in England and Wales. Hydrol. Earth Syst. Sci. 22, 1051–1064. https://doi.org/10.5194/hess-22-1051-2018.

Trenberth, K.E., Jones, P.D., Ambenje, P., Bojariu, R., Easterling, D., Tank, A.K., Parker, D., Renwick, J.A., Adler, R., Alexander, L., Alexandersson, H., Allan, R., Baldwin, M.P., Beniston, M., Bromwich, D., Camilloni, I., Cassou, C., Cayan, D.R., Chang, E.K.M., Christy, J., Dai, A., Deser, C., Dotzek, N., Fasullo, J., Fogt, R., Folland, C., Forster, P., Free, M., Frei, C., Gleason, B., Grieser, J., Groisman, P., Gulev, S., Kripalani, R., Kunkel, K., Marshall, G., Mears, C., Mote, P., Nakamura, H., Nicholls, N., Norris, J., Oki, T., Robertson, F.R., Rosenlof, K., Semazzi, F.H., Shea, D., Shepherd, J.M., Shepherd, T.G., Sherwood, S., Siegmund, P., Simmonds, I., Simmons, A., Thorncroft, C., Thorne, P., Uppala, S., Vose, R., Wang, B., Warren, S., Washington, R., Wheeler, M., Wielicki, B., Wong, T., Wuertz, D., Hoskins, B. J., Karl, T.R., Jallow, B., 2007. Observations: Surface and Atmospheric Climate Change 102.

Troy, T.J., Sheffield, J., Wood, E.F., 2011. Estimation of the terrestrial water budget over northern eurasia through the use of multiple data sources. J. Clim. 24, 3272–3293. https://doi.org/10.1175/2011JCLI3936.1.

van de Giesen, N., Liebe, J., Jung, G., 2010. Adapting to climate change in the Volta Basin, West Africa. Curr. Sci. 98, 1033–1037.

van Huijgevoort, M.H.J., Hazenberg, P., van Lanen, H. a J., Teuling, A.J., Clark, D.B., Folwell, S., Gosling, S.N., Hanasaki, N., Heinke, J., Koirala, S., Stacke, T., Voss, F., Sheffield, J., Uijlenhoet, R., 2013. Global multimodel analysis of drought in runoff for the second half of the twentieth century. J. Hydrometeorol. 14, 1535–1552. https://doi.org/10.1175/JHM-D-12-0186.1.

Van Loon, A.F., 2015. Hydrological drought explained. WIREs Water 2, 359–392. https://doi.org/10.1002/wat2.1085.

Van Loon, A.F., Laaha, G., 2015. Hydrological drought severity explained by climate and catchment characteristics. J. Hydrol. Drought Process. Model., Mitig. 526, 3–14. https://doi.org/10.1016/j.jhydrol.2014.10.059.

Van Loon, A.F., Stahl, K., Baldassarre, G.D., Clark, J., Rangecroft, S., Wanders, N., Gleeson, T., Dijk, A.I.J.M.V., Tallaksen, L.M., Hannaford, J., Uijlenhoet, R., Teuling, A.J., Hannah, D.M., Sheffield, J., Svoboda, M., Verbeiren, B., Wagener, T., Lanen, H.A.J.V., 2016. Drought in a human-modified world: reframing drought definitions, understanding, and analysis approaches. Hydrol. Earth Syst. Sci. 20, 3631–3650. https://doi.org/10.5194/hess-20-3631-2016.

van Oel, P.R., Martins, E.S.P.R., Costa, A.C., Wanders, N., van Lanen, H.A.J., 2018. Diagnosing drought using the downstreamness concept: the effect of reservoir networks on drought evolution. Hydrol. Sci. J. 63, 979–990. https://doi.org/10.1080/02626667.2018.1470632.

Van Tiel, M., Van Loon, A.F., Seibert, J., Stahl, K., 2021. Hydrological response to warm and dry weather: do glaciers compensate. Hydrol. Earth Syst. Sci. 25, 3245–3265. https://doi.org/10.5194/hess-25-3245-2021.

Vicente-Serrano, S.M., Beguería, S., Gimeno, L., Eklundh, L., Giuliani, G., Weston, D., El Kenawy, A., López-Moreno, J.I., Nieto, R., Ayenew, T., Konte, D., Ardö, J., Pegram, G.G.S., 2012. Challenges for drought mitigation in Africa: the potential use of geospatial data and drought information systems. Appl. Geogr. 34, 471–486. https://doi.org/10.1016/j.apgeog.2012.02.001.

Vidal, J.-P., Martin, E., Franchistéguy, L., Habets, F., Soubeyroux, J.-M., Blanchard, M., Baillon, M., 2010. Multilevel and multiscale drought reanalysis over France with the Safran-Isba-Modcou hydrometeorological suite. Hydrol. Earth Syst. Sci. 14, 459–478. https://doi.org/10.5194/hess-14-459-2010.

Wanders, N., Wood, E.F., 2016. Improved sub-seasonal meteorological forecast skill using weighted multi-model ensemble simulations. Environ. Res. Lett. 11, 094007 https://doi.org/10.1088/1748-9326/11/9/094007.

Wanders, N., Wada, Y., Van Lanen, H. a J., 2015. Global hydrological droughts in the 21st century under a changing hydrological regime. Earth Syst. Dyn. 6, 1–15. https://doi.org/10.5194/esd-6-1-2015.

Wang, A., Lettenmaier, D.P., Sheffield, J., 2011. Soil moisture drought in China, 1950–2006. J. Clim. 24, 3257–3271. https://doi.org/10.1175/2011JCLI3733.1.

Wilhite, D.A., Svoboda, M.D., Hayes, M.J., 2007. Understanding the complex impacts of drought: A key to enhancing drought mitigation and preparedness. Water Resour. Manag. 21, 763–774. https://doi.org/10.1007/s11269-006-9076-5.

WMO, 2008. Manual on Low-flow Estimation and Prediction. World Meteorological Organization.

Yevjevich, V.M., 1967. Objective approach to definitions and investigations of continental hydrologic droughts, An.